Title
Mini Implant Facilitated Accelerated Tooth Movement in Rats

Author
Cheung, Tracy Li

Publication Date
2014

Peer reviewed|Thesis/dissertation

UNIVERSITY OF CALIFORNIA

Los Angeles

Mini Implant Facilitated Accelerated Tooth Movement in Rats

A thesis submitted in partial satisfaction of the requirements for the degree Master of Science in Oral Biology

by

Tracy Li Cheung

2014

ABSTRACT OF THE THESIS

Mini Implant Facilitated Accelerated Tooth Movement in Rats

by

Tracy Li Cheung
Master of Science in Oral Biology

University of California, Los Angeles 2014
Professor Christine Hong, Chair

Objective: Accelerated tooth movement (TM) is achieved in orthodontics via corticotomy (CY) but with invasive surgical interventions. Minimally invasive CY using mini-implant may expedite TM. In this study, we developed a rat model to evaluate orthodontic TM with mini implant-assisted CY.

Methods: A split-mouth experimental design was utilized in six Sprague-Dawley rats with the CY left side and the sham right side of the maxillary 1st molars. 25g close-coiled springs were secured to both incisors and 1st molars. TM was observed by diastema measurement. Samples were analyzed by MicroCT, H&E and TRAP.

Results: Compared to the sham side, the CY side exhibited 30% greater TM, 10% greater BMD and 7% greater BV/TV. More osteoclasts were found in the CY side; 44% and 55% more in the total alveolar bone and pressure side bone, respectively.

Conclusions: Non-surgical method of CY using mini implant shortened TM and improved bone quality, demonstrating that the modified mini implant-assisted CY may shorten orthodontic treatment time.

The thesis of Tracy Li Cheung is approved.

Reuben Kim

Xinli Zhang

Christine Hong, Committee Chair

TABLE OF CONTENTS

A: INTRODUCTION 1

A1: Preface and Specific Aims 1

A2: Biology and Biomechanics of Tooth Movement 4

A3: Regional Acceleratory Phenomenon 5

B: PURPOSE 7

B1: A Modified Mini-implant Driver: A non-surgical corticotomy tool 7

B2: Previous and Current Accelerated Tooth Movement Techniques 8

C: APPROACH 10

C1: Introduction 10

C2: Subjects 11

C3: Sedation and Pain Control 11

C4: Treatment 12

C5: MicroCT Protocol and Analysis 14

C6: Histological Analysis 35

D: RESULTS 37

D1: Statistical Analysis 36

D2: In-vivo Measurements 36

D3: MicroCT Analysis 37

D4: Histological Analysis 37

E: DISCUSSION 38

F: CONCLUSIONS 45

G: FIGURES 46

H: BIBLIOGRAPHY 57

LIST OF FIGURES

Figure 1:	New theory of orthodontic tooth movement	46
Figure 2:	Corticotomy placed in alveolar bone	46
Figure 3:	Rat with orthodontic appliances	47
Figure 4:	Osteoclast quantification	48
Figure 5:	Iatrogenic pulp exposure	48
Figure 6a:	Diastema change	49
Figure 6b:	Average diastema change	49
Figure 7:	MicroCT evaluation of corticotomies	50
Figure 8a:	BV/TV analysis	50
Figure 8b:	Average results for BV/TV analysis	51
Figure 9a:	BMD analysis	51
Figure 9b:	Average results for BMD analysis	52
Figure 10a:	Corticotomy side H&E	52
Figure 10b:	Control side H&E	53
Figure 11:	Corticotomy vs. control side bone	53
Figure 12:	New bone quantification	54
Figure 13a:	Osteoclast quantification for alveolar and intraradicular bone	54
Figure 13b:	Average osteoclast quantification for alveolar and intraradicular bone	55
Figure 14a:	Osteoclast quantification for pressure side	55
Figure 14b:	Average osteoclast quantification for pressure side	56

ACKNOWLEDGEMENTS

I would like to thank Dr. Christine Hong for giving me the opportunity to be in her first cohort of lab members. I enjoyed being able to oversee my project from start to finish, and execute all the steps in between. What a great learning experience!

There were many experts who contributed to my understanding of my project. I would like to thank Dr. Kang Ting, Dr. Won Moon and Dr. Gregory Lawson for their guidance. I would also like to express gratitude to Dr. Reuben Kim and Dr. Xinli Zhang for giving their time to be on my thesis committee.

Teamwork is essential to the success of any project. I would like to thank Dr. Juyoung Park and Mr. Raymund Rebong for working alongside me until the 11th hour.

Finally, I rely on two very special individuals their love and support. Therefore, I would like to thank Mr. Clifford Matthews Baum, my husband, and Dr. Lillian Tsai Li, my mother, for always making sure that my cup is half full.

A. INTRODUCTION

A1: Preface and Specific Aims

Orthodontic treatment helps individuals suffering from malocclusion by achieving proper dentofacial form and function. However, many patients are concerned with the social discomfort associated with wearing braces and the time commitment required, such as treatment length and the sheer number of appointments. The current techniques for accelerated tooth movement (ATM) are invasive and often involve surgery. Such methods also require concomitant treatment by a periodontist and an orthodontist, which may pose a financial and logistical burden for the patient. We aim to develop a minimally invasive tool and protocol that minimizes risk while maximizing efficacy and efficiency of the orthodontic treatment for the patient.

There are significant dental and periodontal complications associated with lengthy orthodontic treatment. External apical root resorption is known to be correlated with the duration of active orthodontic treatment (65). Additionally, fixed orthodontic appliances can trap plaque and increase plaque index (20). Consequently, reports have linked patients with fixed orthodontic appliances with an increased level of dental caries and subsequent gingivitis (59) and loss of periodontal support (21). In attempts to address these concerns by reducing treatment time, the techniques of corticotomy with burs (62), piezocision (13) and mallets (44) have been developed. However, these procedures are often invasive and require concomitant periodontal surgery, and corticotomy has been associated with adverse effects on the periodontium, including loss of attached gingiva, interdental bone loss (37), and periodontal defects such as reduction in alveolar bone height (16). Subcutaneous hematomas of the face and neck are also attributed to corticotomies combined with periodontal surgery (43).

When patients request expedited treatment, clinicians usually suggest the standard technique of raising a flap and creating corticotomies, despite the inherent risks that come with invasive procedures. We aim to develop a minimally invasive method that does not involve periodontal surgery. This technique will be less traumatic when compared to other corticotomy techniques such as periodontally assisted osteogenic orthodontics and cortical incision. Equipped with such a treatment modality, orthodontists may be able to significantly shorten treatment time and reduce discomfort, compared to current ATM techniques. In our study, we developed and tested a modified mini implant driver as an effective tool for creating corticotomies without the need to raise flaps. We tested the hypothesis that ATM can be accomplished in a minimally invasive manner that requires no more than local infiltration for pain management.

AIM 1: To modify a mini implant driver for producing consistent corticotomies

In AIM 1 we will modify a conventional mini implant driver to create corticotomies of controlled depth and size. Notable advantages of the mini implant driver are that it is 1) portable as it does not require auxiliary attachment lines, 2) operated without the need for batteries and 3) does not require a cooling mechanism as the tool is hand-driven and will not achieve temperatures sufficient to cause any cauterization of the gingiva or bone.

Primary outcome measures: Successful in-vivo creation of corticotomies of specific depth, size, with minimal force and without flap surgery. **Success Criteria:** Development of a tool that fulfills the primary outcome measures.

AIM 2: To develop a protocol for orthodontic tooth movement in rats

In AIM 2, we will develop a split-mouth design for orthodontic tooth movement in rats. The orthodontic appliance should be ligated to the maxillary first molar and central incisor and allow the molar to move mesially. The appliance should be able to be fitted on the right and left sides of the maxilla. The forces used for space closure should be consistent.

Primary outcome measures: An orthodontic appliance that is stable throughout the experimental time period. **Success Criteria:** Successful placement of orthodontic appliances that are stable and do not interfere with the rats' ability to eat.

AIM 3: Evaluate if mini implant facilitated corticotomy enhances the rate of tooth movement in a rat study

In **AIM 3**, we will use the modified mini implant driver optimized in **AIM 1** and the protocol developed in **AIM 2** to complete a split-mouth study in rats with an experimental period of three weeks. Tooth movement will be measured intraorally with a digital caliper. MicroCT analysis will be used to evaluate bone mineral density (BMD) and bone fraction (Bone Volume/Tissue Volume). Histological analysis will include: H&E for histomorphometric description, TRAP for osteoclast quantification.

Primary outcome measures: Success placement of corticotomies in-vivo using modified mini implant driver devised in **AIM 1. Success Criteria:** Observation of increased tooth movement on the corticotomy side versus the control side supported by in-vivo measurements, microCT and histological analysis.

A2: Biology and Biomechanics of Tooth Movement

In order to understand how corticotomies accelerate tooth movement, a review of biology and biomechanics of tooth movement is necessary. The theory of tooth movement has been debated since 1815 (11). Today, clinicians accept the premise that prolonged pressure on teeth causes the alveolus to remodel and allow teeth to move {Masella, 2006 #1}. Existing bone is resorbed in areas of pressure and new bone is formed in areas of tension. Currently, the accepted sequence of biological events for bone remodeling and subsequent tooth movement on the pressure side is: 1) inflammation and blood flow alteration, 2) periodontal ligament (PDL) cell necrosis, 3) macrophage-initiated phagocytosis of necrotic cells, and 4) osteoclasts in areas of hyalinization resorbing bone resulting in undermining resorption (46). Today, it is debated as to whether bone resorption and deposition is confined to discrete compartments; rather, these two dynamic processes can occur at any point in the alveolar bone adjacent to the tooth (**fig. 1)** (23, 24). On the tension side blood flow is enhanced followed by increased osteoblastic activity and bone deposition, which results in increased mineralization. MMP-9 has been shown to be the main protease produced by active osteoclasts (42) and is responsible for their invasive activity (12). The purpose of bone remodeling is to repair damage due to force or trauma. The rate of bone resorption controls the rate of tooth movement, and osteoclast activity facilitates bone turn over.

The biomechanics of orthodontic tooth movement has also been controversial. A systematic review of optimum force magnitude and temporal characteristics found that there is no agreed upon ideal force magnitude (light vs. heavy) or temporal characteric (intermittent vs. continuous) to produce the greatest rate of tooth movement (48). The PDL has an intrinsic force that must be overcome in order for tooth movement to occur (50). This can be seen clinically

when diastema and drifting of teeth occur in individuals with periodontal disease (8). This observation is due to the weakened PDL fibers and their reduced ability to resist forces from mastication and orofacial muscles. The two proposed theories of tooth movement are: 1) biomechanical and 2) combined bone bending, piezoelectric forces and magnetic forces (46, 50). The biomechanical theory states that distortion of cells in the periodontal ligament stimulate the production of prostaglandins, which ultimately stimulate osteoblasts to lay down bone at the tension side and osteoclasts to resorb bone at the pressure side**.** "Positive strain" on the tension side of the PDL leads to bone deposition and "negative strain" on the pressure side leads to bone resorption (23). In the other theory, three simultaneous forces, 1) bone bending, 2) piezoelectric force and 3) magnetic force, produce tooth movement. Distortion of the bone generates small electrical potentials, which may link bone changes with electrical forces. Piezoelectric forces are created any time there is distortion of a crystalline structure, which has been demonstrated in dry bone manipulation. However, piezoelectric forces alone do not account for orthodontic tooth movement because in in vivo tissues, nerve impulses and their subsequent action potentials create larger electrical fields (40). Magnetic fields may increase the rate of tooth movement (9), but magnets alone are unlikely to be the sole reason behind orthodontic tooth movement. Finally, PDL bending cannot account for all orthodontic tooth movement, as the tooth moves more than the PDL width. Therefore, some degree of bone bending must occur to accommodate movement (50).

A3: Regional Acceleratory Phenomenon (RAP)

In 1959, Kole pioneered the corticotomy technique (36) to accelerate orthodontic tooth movement, where he made "wedge shaped crestal ostectomies" (41) through the alveolus. He

believed that these surgically created bony blocks would eliminate the resistance of the cortical bone and facilitate tooth movement (34-36). Corticotomy is defined as surgical cuts or perforations into the cortical bone, leaving the medullary bone intact. Today, it is believed that accelerated tooth movement (ATM) is not due to gross movement of bony blocks but rather to "Regional Acceleratory Phenomenon (RAP)" (38), a term coined by Frost, an orthopedic surgeon (18), which describes the benefits of decortication—a form of mechanical trauma—in bone repair. In RAP, teeth move faster through areas of demineralized bone than through mineralized bone. The theory proposes that decortication initiates the normal bone healing events with enhanced medullary bone remodeling in areas adjacent to the mechanical trauma (51). Studies in rabbits have demonstrated a five-fold increase in bone remodeling under RAP compared to controls (6) and that the replacement medullary bone is lower in density as well, which helps to expedite tooth movement rate (60). Corticotomy **(fig. 2)** is one such way of stimulating the bone to cause inflammation, which initiates the process of demineralization (38). This process is in contrast to what occurs following an osteotomy, in which cuts are made not only into cortical bone, but through the medullary bone, as well. Immediately following osteotomy, hematoma and granulation tissue formation occur in the reactive phase. In the reparative phase, a flexible callus forms, which is eventually replaced by immature woven bone and is finally remodeled into lamellar bone. The entire process of bone healing and remodeling can take up to eighteen months, but bone is 80% healed at three months. In corticotomy, theoretically there is demineralization, rather than loss of bone. There is no callus formation during RAP. The benefits of corticotomy-assisted tooth movement include lack of hyalinization (25). In 2008, Sebaoun et al. found that decortication in the maxillary buccal and lingual alveolus resulted in a three-fold greater catabolic activity (osteoclast number) and anabolic activity (bone

deposition), which supports the interplay of demineralization and remineralization found in RAP (52), and opens the possibility of an increase in bone fraction relative to baseline. When RAP occurs, there is an earlier onset of osteoclastogenesis, and therefore and earlier onset of bone turnover (5). In order to understand the profound effect osteoclasts have on bone remodeling, a discussion of the molecular events leading to osteoclastogenesis is needed. Orthodontic forces induce mechanotransduction via cytokines. The primary cytokines involved with recruitment, differentiation, activation and survival of osteoclasts are RANKL and M-CSF, which are expressed by osteoblasts. RANKL and M-CSF bind to RANK and c-Fms, which are expressed on osteoclast precursors and mature osteoclasts. Orthodontic force downregulates OPG expression by osteoblasts. OPG competitively binds to RANKL to reduce RANK/RANKL interactions. RANKL expression is further upregulated by PGE_2 and IL-1β synthesis (3).

B. PURPOSE

B1: A Modified Mini-implant Driver: A non-surgical corticotomy tool

Adults seeking orthodontic treatment are often concerned with efficiency of treatment and may refuse orthodontic treatment due to length of treatment, number of appointments and social discomfort associated with the presence of braces. There are also dental and periodontal risks associated with orthodontic treatment. External apical root resorption is a possible sequela of comprehensive orthodontic treatment and can be minimized with use of light forces and efficient treatment duration (65). Additionally, fixed orthodontic appliances serve as crevices for bacterial growth and can cause periodontal inflammation. To address some of these issues, surgically facilitated techniques have been developed to accelerate treatment. Various methods of corticotomy have been reported in the literature using burs (62), piezocision (13) and mallets

(44). However, these procedures are not without risks, including bruising, ecchymosis and edema. In light of the current limitations, development of a non-surgical tool and protocol that minimizes risk and maximizes efficacy and efficiency for the patient is necessary. With this new protocol, orthodontists will be able to satisfy the patient's desire for significantly shorter treatment time with a reduction in the discomfort experienced with surgically-facilitated ATM.

Since it has already been proven that ATM can be accomplished via mechanical trauma to the cortical bone, the basis for the design of this new tool is one that facilitates corticotomy placement in a minimally invasive manner that eliminates the need for initial flap surgery.

B2: Previous and Current Accelerated Tooth Movement Techniques

A review of the existing techniques has confirmed that our corticotomy technique recommendation is innovative. Rathbun et al. (1986, 1990) elevated mucoperiosteal flaps on the buccal and lingual and then scored the cortical bone with vertical and horizontal grooves. Orthodontic treatment commenced immediately after surgery (4, 19). In 1998, Drs. Thomas and William Wilcko invented accelerated osteogenic orthodontics, coined "Wilckodontics." In this technique, a periodontist raises a split thickness flap, leaving a gingival collar, and decorticates the bone with a round bur (41). In 2006, Dr. Young Guk Park used a mallet to hammer a surgical blade through the gingiva and into the alveolar bone (44). However, this technique does not offer the increase in bone volume associated as there is no bone graft and some patients may find this technique to be aggressive. Additionally, dizziness has been reported after the use of osteotomes (45). Dibart et al. (2009) modified the Wilckos' technique, creating a method in which a surgical blade is used to make cuts into the gingiva and a piezoelectric knife is used to penetrate 3mm into the buccal cortex (13). Although periodontal surgery combined with various methods of

mechanical trauma unquestionably expedites treatment time, concerns regarding morbidity cannot be dismissed. Complications associated with any surgical procedures include hypovolemia, post-operative pain, infection, delayed wound healing and necrosis and dehiscence. This is by no means an exhaustive list of risks inherent with surgery, but these examples justify the need for a technique with fewer potential complications. It has been long known that raising partial or full thickness flaps opens the possibility of alveolar bone height reduction (63), and thus there is an urgency to establish techniques that are safer for long-term periodontal health. The popularity of the current techniques may be limited due to the aforementioned iatrogenic effects (7).

Novel non-mechanical techniques such as local administration of 1,25 dihydroxycholecalciferol, prostaglandin E2 (27, 29) and irradiation with a Ga-Al-As diode 810 nm (17, 64), 830 nm (30) and 623.8 nm lasers (55) in an animal model have demonstrated accelerated tooth movement. Another study using pulsed Optodan 850 nm and continuous KLO3 630 nm lasers found that when subjected to laser treatment, teeth moved less than in controls (53), which suggests that certain wavelengths are capable of inducing the appropriate environment for accelerated tooth movement while others are not. Continuous administration of parathyroid hormone was demonstrated to accelerate tooth movement in rats (54). The receptor activator of nuclear kappa B ligand (RANKL) expression was also increased in the compression side of the bone. In 2006, Kanzaki et al. showed that transfer of RANKL gene to periodontal tissue increased the rate of tooth movement (28). Administration of BMP-2 reportedly slows down corticotomy-assisted tooth movement (24). Although non-mechanical techniques show promise in literature, their clinical efficacy is not as well-established as mechanical techniques.

C. APPROACH

C1: Introduction

Our goal was to evaluate if mini implant-facilitated corticotomy enhanced the rate of tooth movement in a rat study. Rats underwent anesthesia and were subjected to split-mouth orthodontic treatment. On one side of the mouth, a 1.2 mm diameter 6 mm length mini implant (BMK, South Korea) was used to puncture through rats' soft tissue and into the bone mesial and palatal to the first maxillary molar. We used an automatic implant driver to calibrate the rotations to 30 rpm and the torque to 90 Ncm. The maximum depth of penetration was 1 mm (0.5 mm to account for the soft tissue, and .5 mm to penetrate through the cortical bone). Treatment lasted three weeks, a duration that has been shown to be effective in studying orthodontic tooth movement (49). It takes anywhere between a few days and a couple of weeks to reach the "linear phase", where the majority of tooth movement occurs (46). A previous study showed that the rate of tooth movement sharply decreased on Day 14 and Day 21 for tooth movement and tooth movement + corticotomy groups, respectively. The greatest rate of tooth movement occurred between Days 1 and 7 and Days 7 and 14 for tooth movement + corticotomy and tooth movement only groups, respectively (5). At the end of the study, the rats were humanely euthanized and tissue samples were harvested for further analysis. Although several animal species could serve as models for orthodontic tooth movement, rats were selected for several reasons. The dentition of rats is an appropriate model for our study because, like their human counterparts, rats have incisors, premolars and molars. There are also natural spaces between the rat's teeth that allow for space closure without prior extraction of teeth. Although dogs are a good model for tooth movement as their bone quality resembles that of humans (1), initial extraction of premolars is needed to create an appropriate model for space closure (47). The fresh

extraction sites may act as regions of demineralization, which could confound the effects of corticotomy. A systematic review of corticotomy-assisted orthodontic tooth movement shows that space closure was commenced immediately after extraction (22), and so it might be difficult to differentiate whether the cause for the accelerated tooth movement is due to corticotomy or to extraction. We avoid this confounding factor in rats as extractions are not needed. Finally, the rat's jaw, although small and limited in maximum opening, can open adequately for placement of orthodontic appliances.

C2: Subjects

Six male Sprague-Dawley rats (500g) were administered split-mouth mini implant (MI) facilitated corticotomy to enhance tooth movement for 21 days (3 weeks). The Wilcoxon Rank Sign Test was used to determine the number of animals needed. Split-mouth refers to the fact that both sides of the maxilla will receive orthodontic force application but only one side will receive corticotomies. All rats were euthanized at 21 days with CO_2 asphyxiation and their maxillae were harvested for MicroCT analysis, histologic staining and examination. This allowed us to evaluate whether there were any differences in the bone condition of rats that received the corticotomy intervention. Tooth movement measures were taken in-vivo on Day 0 and Day 21 using a digital caliper. The protocol was approved by the University of California, Los Angeles Animal Research Committee.

C3: Sedation and Pain Control

Prior to surgery and orthodontic appliance placement, sedation of rats was initially accomplished with inhaled isoflurane. Once the animal was unconscious, we administered IP

ketamine/xylazine (75-85 mg/kg for induction, 5-10 mg/kg for maintenance) to induce and/or continue anesthesia. Although the surgery was minimally invasive and minimal bleeding was anticipated, SC buprenorphine (.01-.05 mg/kg, volume 20 ml/kg maximum) was administered pre-operatively and post-operatively every 8 hours for 48 hours to alleviate any discomfort.

C4: Treatment

The rat's maxilla consists of one incisor and three molars on the right and left sides. Our orthodontic appliance was designed such that the first maxillary molar was protracted mesially with a 25 g Sentalloy closed coil spring (GAC International, NY) using the maxillary incisor as anchorage (**fig. 3)**. The maxillary incisor was an ideal near absolute anchorage unit as the root is extremely long and curved. The planned placement of the corticotomies into the cortical bone was just mesial to the first molar and on the palatal aspect of the alveolar bone housing the tooth, as we wished to concentrate the decortication to the areas in which we hoped to see tooth movement. The surgical procedure involved puncturing the rat gingiva and cortical bone to a maximum depth of 1 mm using a mini implant affixed to an automated slow-speed implant driver at 30 RPM. We calibrated the depth by marking the height on the implant with surgical tape. This ensured that the implant did not penetrate beyond the necessary depth. It is important to note that the implant did not remain in the rat's jaw and the only purpose of the implant was to create corticotomies. Five corticotomies were placed 1-3 mm apart. No corticotomies were placed on the control side. Mini implant placement in rats resulted in minimal bleeding At most, pressure with cotton pellets provided hemostatic control.

In order to maximize protraction of the posterior unit, only one molar was included in the anchorage unit. This created the largest differential in anchorage value between the molar and the incisor. We took advantage of the fact that the rat maxilla has a large, anatomic, diastema

between the molars and the incisors, which made it an ideal model for space closure. An important consideration in orthodontic appliance placement in rats is that their incisors erupt continuously. As such, appliances were checked daily and re-secured as needed. The first maxillary molar has a natural undercut on its distal interproximal surface, which helped to maintain appliance security. A retention groove was made using a high-speed handpiece on the mesial aspect of the molar to assist in securing the appliance. A second retention groove was placed on the facial surface of the maxillary incisor, approximating the cemento-enamel junction and wrapping around to the distal surface of the tooth. A thin, .09" stainless steel wire was bent and adapted to encircle the first maxillary molar on one side. Wires were also bent to encircle the incisors.. The aforementioned steps were performed on both the CR and CY sides. Additional stability of the wires was achieved by bonding the wires into the retention grooves with bis-GMA composite resin. The purpose of the wire encircling the teeth is two-fold: 1) to encircle the teeth discussed above for anchorage and 2) to ligate the nickel-titanium closed coil spring. These nickel-titanium (Sentalloy) springs are manufactured to provide a consistent force of 25 g throughout activation. The benefit of nickel-titainum was that no adjustment of spring tension was needed during treatment. This helped to ensure that if appliances needed to be re-secured during the experimental period that the amount of force would remain consistent. 25 g spring was the lightest commercially available spring recommended in literature for tooth movement in rats.

Care was taken to not alter the rats' occlusion with the orthodontic appliance. The height of the appliance after placement was below the rat's occlusal plane and no bonding material was placed on the occlusal or incisal surfaces of the teeth. In addition to cautions taken to maintain

the existing occlusion, soft diet was used to minimize appliance disturbance. Normal rat food was mixed with warm water to create a familiar tasting but soft consistency.

One of the disadvantages of feeding the rats soft food was that the rats were not be able to naturally grind their incisors to maintain their length. This required us to check the incisor length daily and file the edges down as needed. Rats were also weighed three times in first week after surgery and then twice-weekly thereafter to ensure that they did not lose more than 5% of their weight. If weight loss ever exceeded 10%, we planned to provide them with a supplemental diet (i.e. high-calorie foods, like peanut butter). At 21 days, the animals were sacrificed and the maxillas were harvested and fixed in 10% buffered formalin.

C5: MicroCT Protocol and Analysis

Rat maxillas were scanned using SkyScan (Bruker Micro CT, Belgium) and analyzed using their proprietary software, CTAn, to evaluate differences in BMD and BV/TV between corticotomy and control sides. We established a step-by-step protocol for analysis:

1. Create a new folder on a PC titled **skyscan**. Save it in the computer's **C drive** so that the folder location is **C:\skyscan**
2. The CTAn + CTVol software is downloaded from http://www.skyscan.be/products/downloads.htm

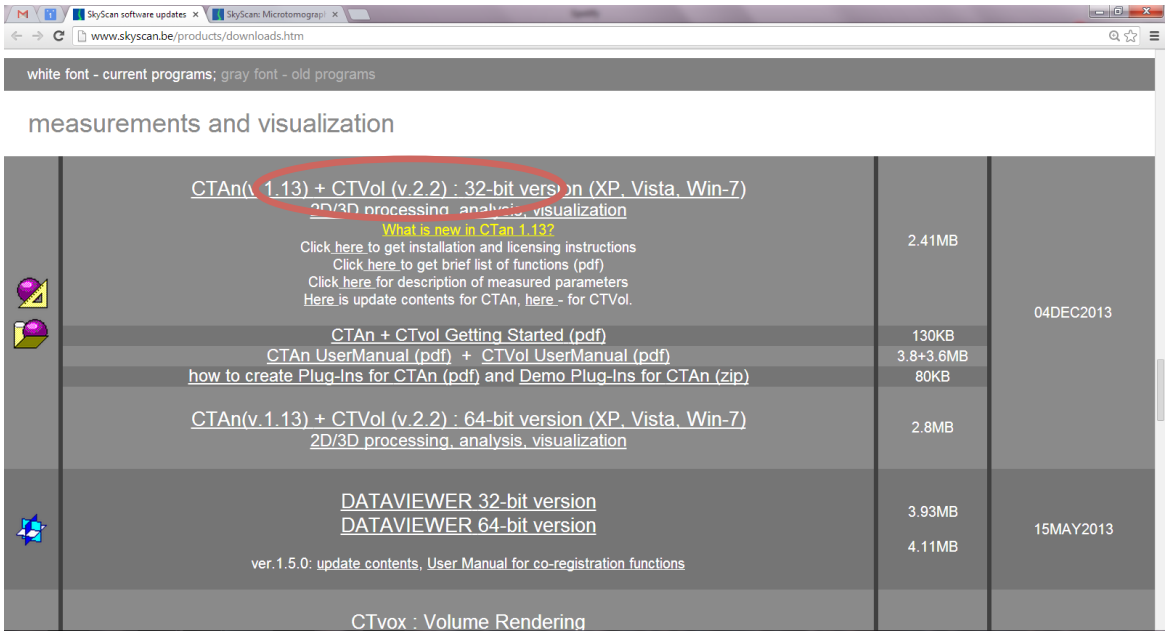

3. Extract all the zipped files from the CTAn + CTVol download and place them into the same new folder **(c:\skyscan).** For example **ctan.exe** should be located in the folder **c:\skyscan**

4. In CTAn, select the **Open Image or Dataset** icon.

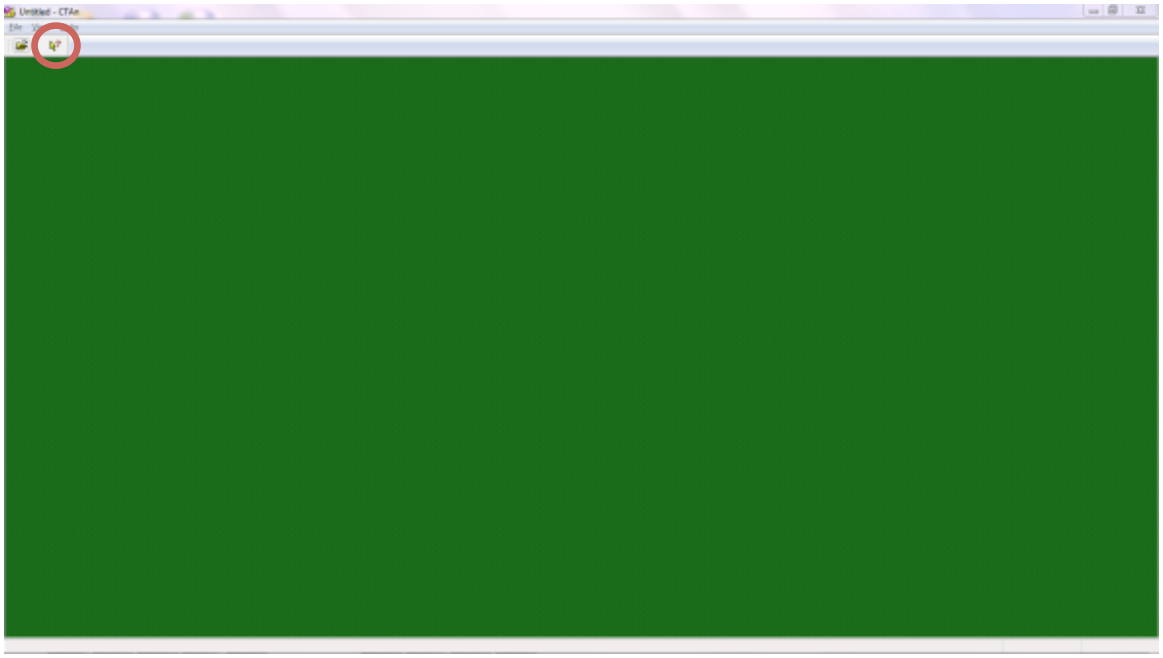

5. Open the folder containing the **.bmp images** of the scanned sample and double click on one image. CTAn will automatically load all the pictures in its program.

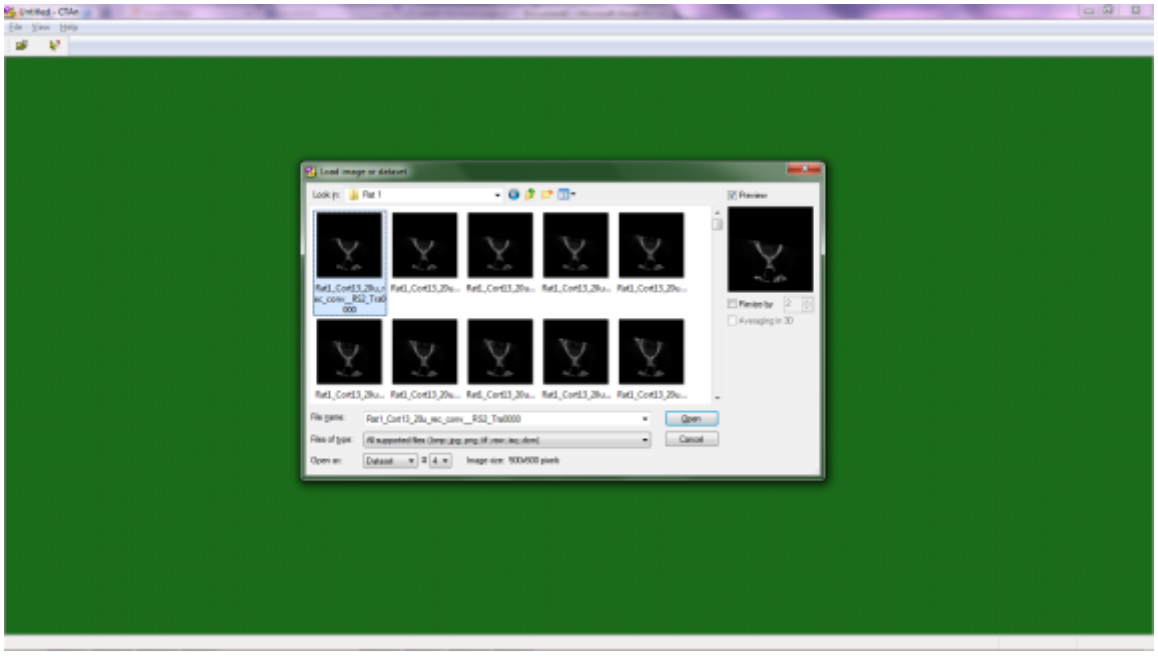

6. Load all the .bmp images into the CTan software and view under the **Raw Images** tab. Each image represents an individual slice of the sample.

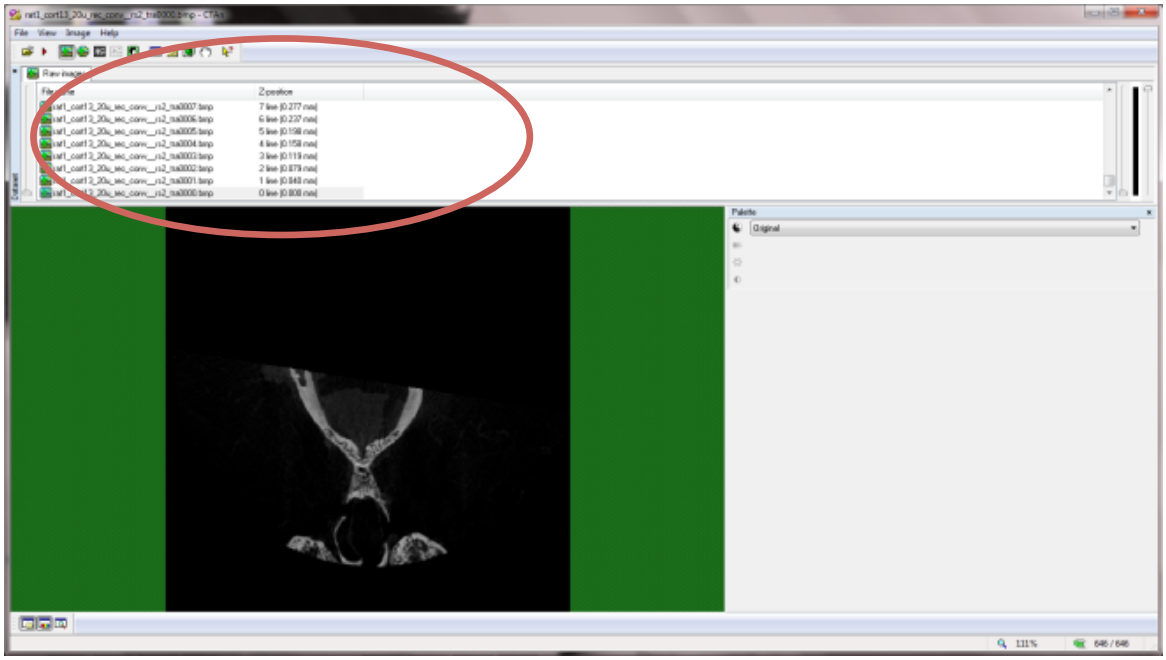

7. Scroll through the slices until the beginning of the region of interest is located. In these datasets, the slices are ordered posteriorly to anteriorly, so that the starting slice is the alveolar bone surrounding the distal aspect of the maxillary first molar. In order to evaluate the slice more carefully, right click anywhere on the image and click **zoom**. The zoom function can be set to any amount, and in this case, 222% is the optimum zoom needed to view the slices with clarity.

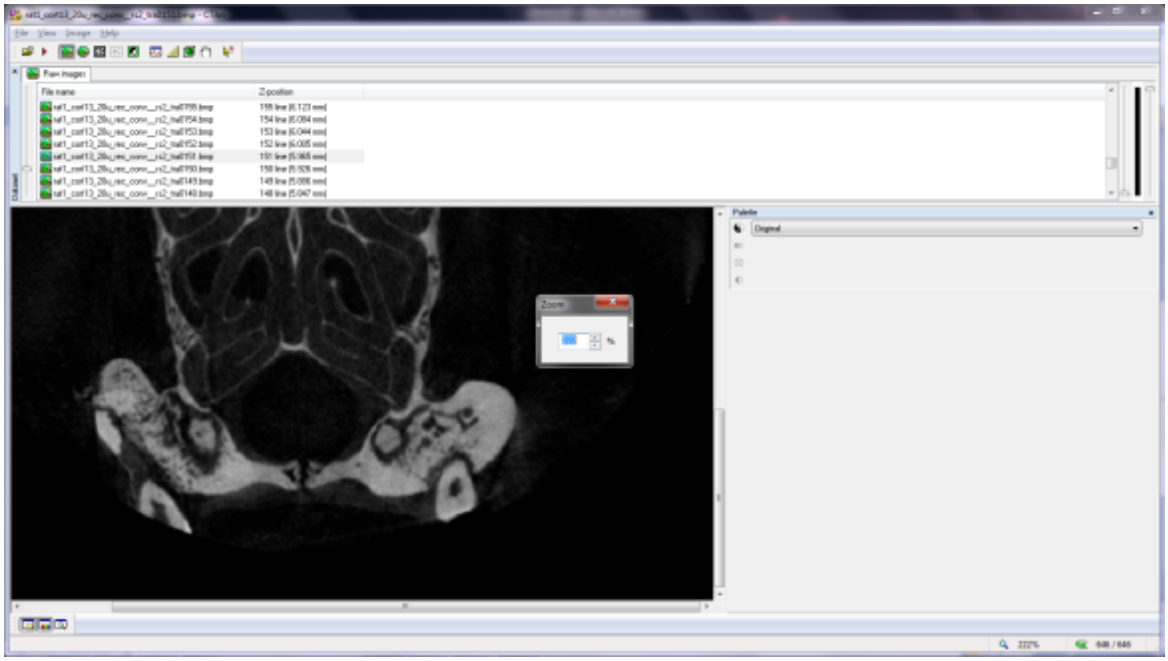

8. Using the **hand mode** icon, the image can now be clicked and dragged in order to center the maxillary first molar on the screen. The image should be dragged so that the tooth and alveolar bone area could be visualized. Unclick the hand icon when reorientation is completed.

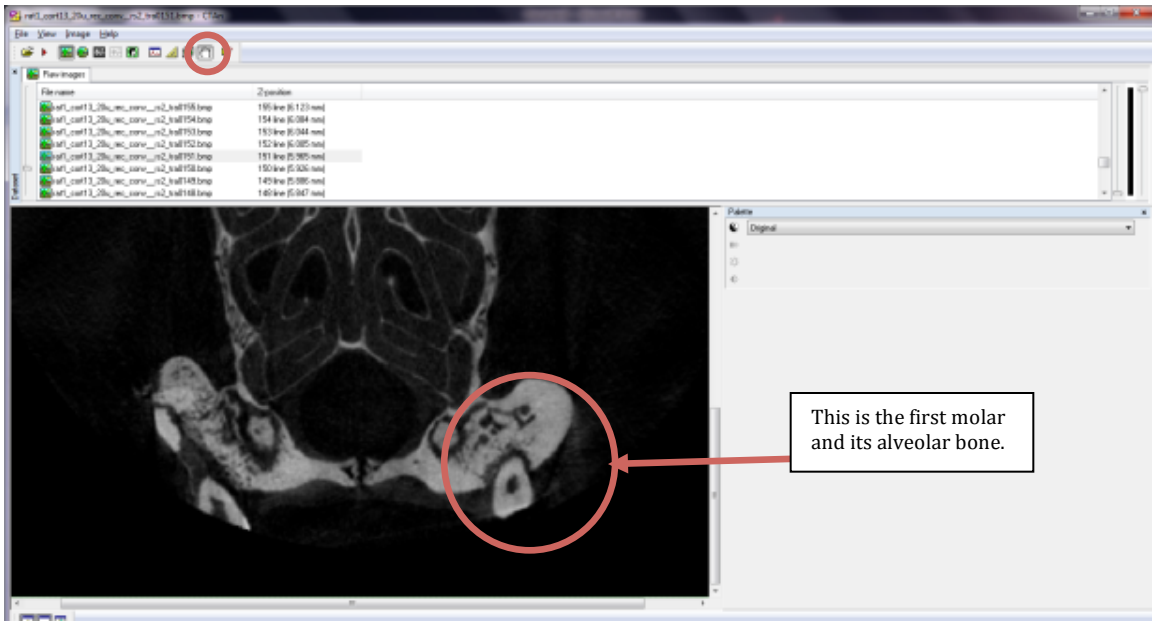

9. Scroll through the slices until the slice containing most mesial portion of the first molar is identified. This point is referred to as the **mesial limit**, which is the image that contains the last sign of radioopaque tooth structure in the alveolar bone.

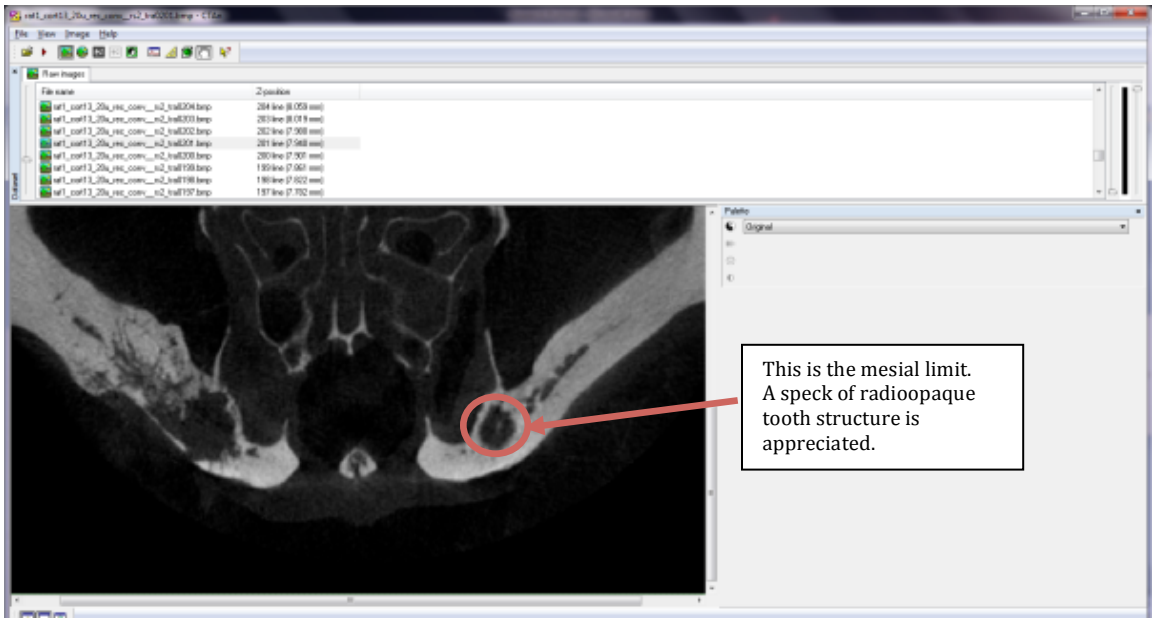

10. Move the scroll bar on the far right until the image with the mesial limit is located. In the **Raw Images** tab, the images before the mesial limit should be grayed out.

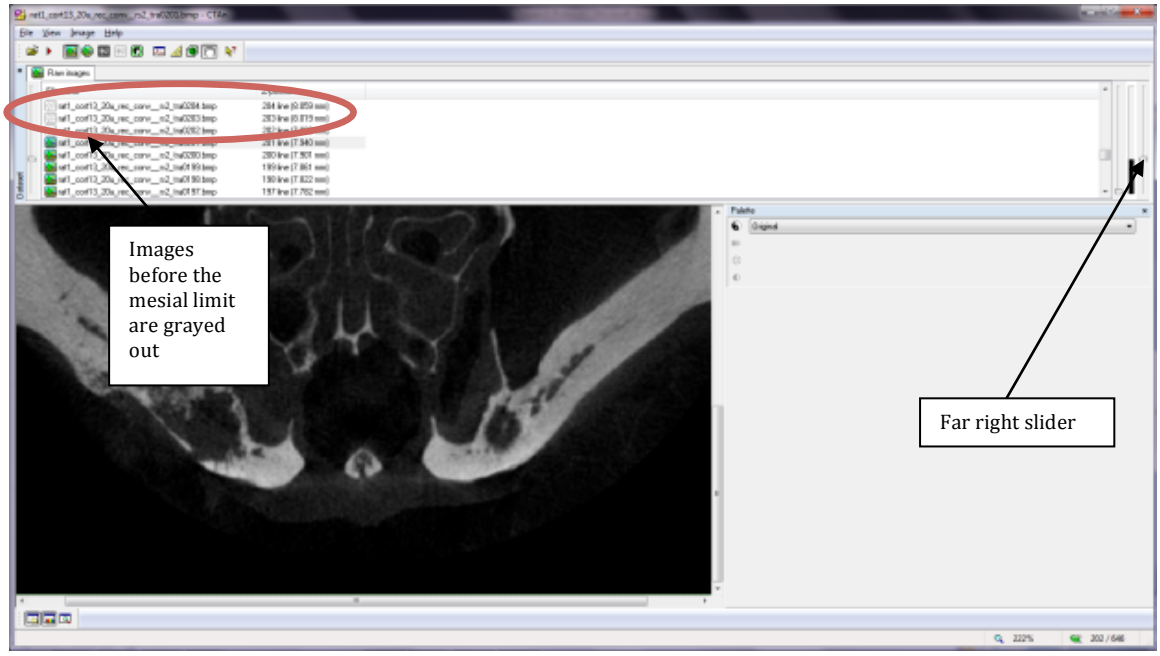

11. Include 3 slices beyond the mesial limit as a buffer in case there are images before the determined mesial limit, including the tooth structure of the first molar. This is considered the **starting point** of the MicroCT analysis.

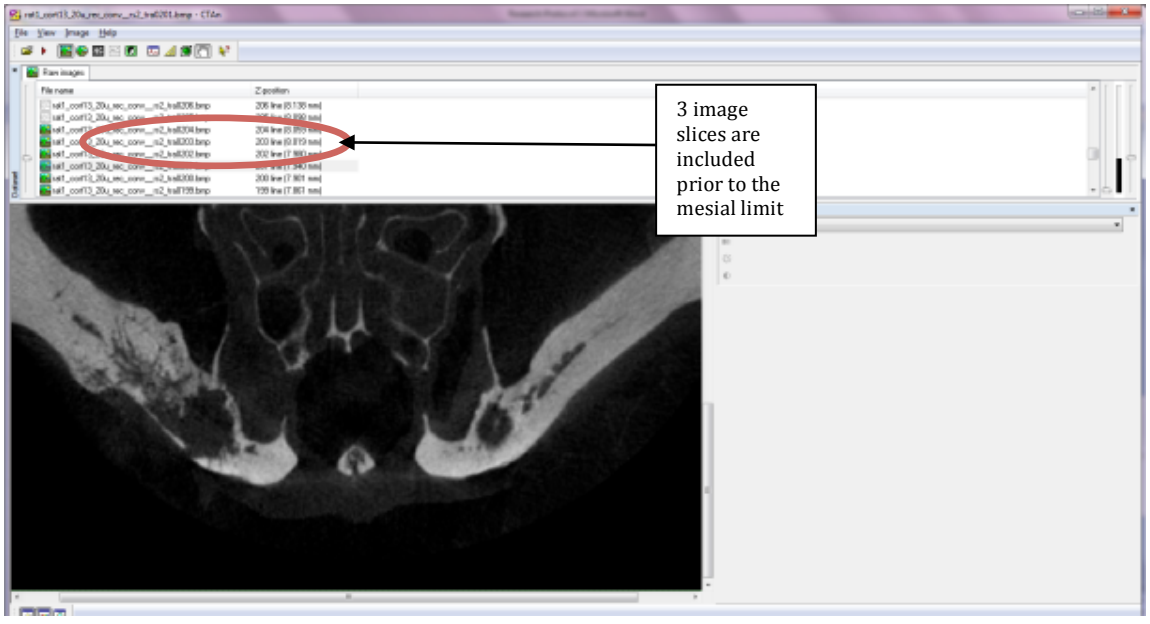

12. Next, scroll through the raw images until the image with the most distal portion of the first molar is identified. This most distal portion of the first molar is referred to as the **distal limit**. This point shows the image containing the first sign of radioopaque tooth structure.

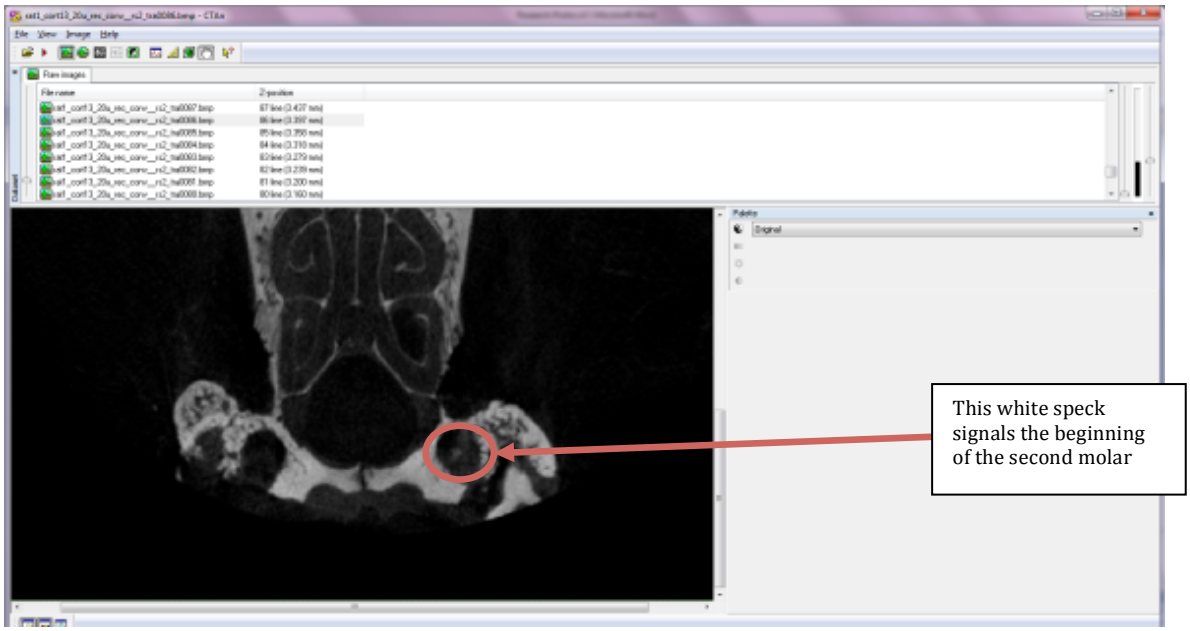

13. Move the far right slider until the image with the distal limit of the first molar is visualized. In the **Raw Images** tab, the images after this slice should be grayed out.

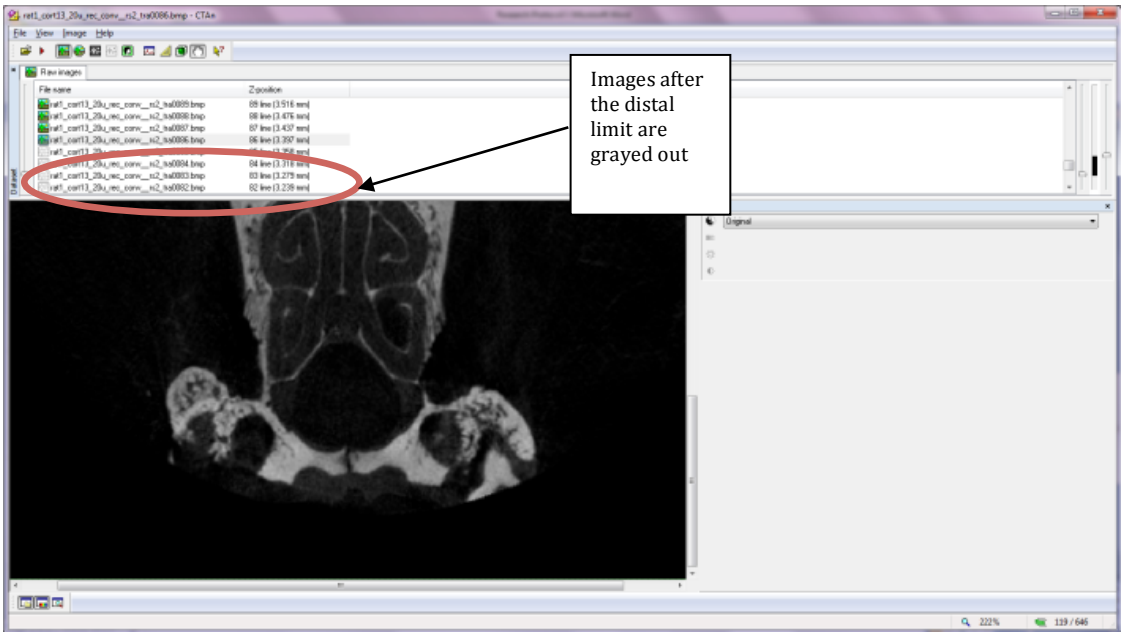

14. 3 images after to the distal limit are included as a buffer in case there are slices after the distal limit that include the tooth structure of the first molar. This represents the **<u>end point</u>** of the microCT analysis. None of the grayed out images beyond the distal limit are included in the data analysis. Setting the mesial and distal limits ensure a consistent methodology of only analyzing the first molar alveolar bone.

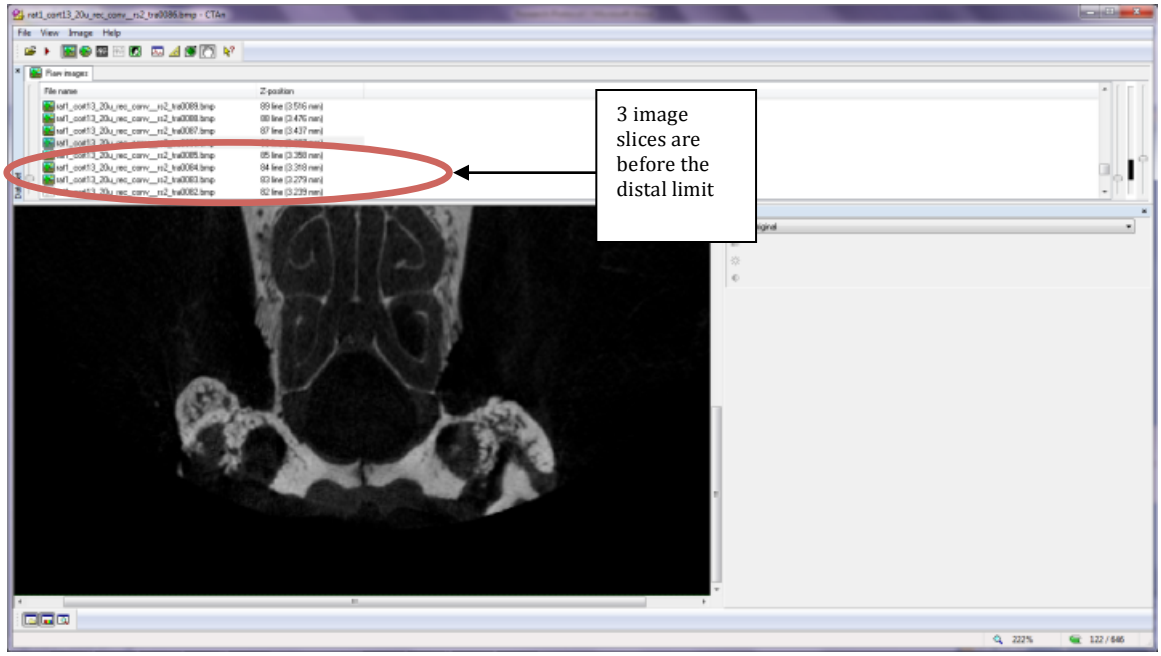

15. The slices are scrolled through until the buccal root of the first molar is idenfied. The buccal root is the smallest of the 5 roots of the first molar (MB, MP, B, DP, DB root). This gives the best representation on the slice of where the buccal bone is least variable. The slices are evaluated until the slices are identified in which the buccal bone appears to be most stable.

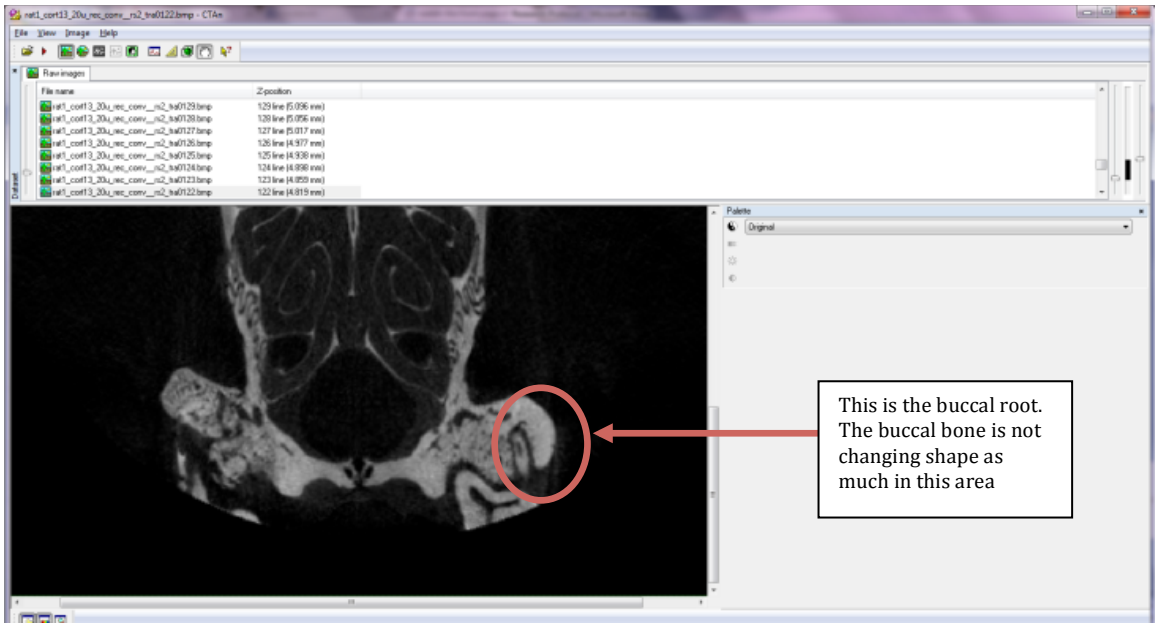

16. Click on the **Measure Tool**. Next click the **Coordinate Tab**. Using the pointer, click the buccal bone at the point of its greatest curve or greatest convexity. The

coordinate selected should appear in the Measure Tool window.

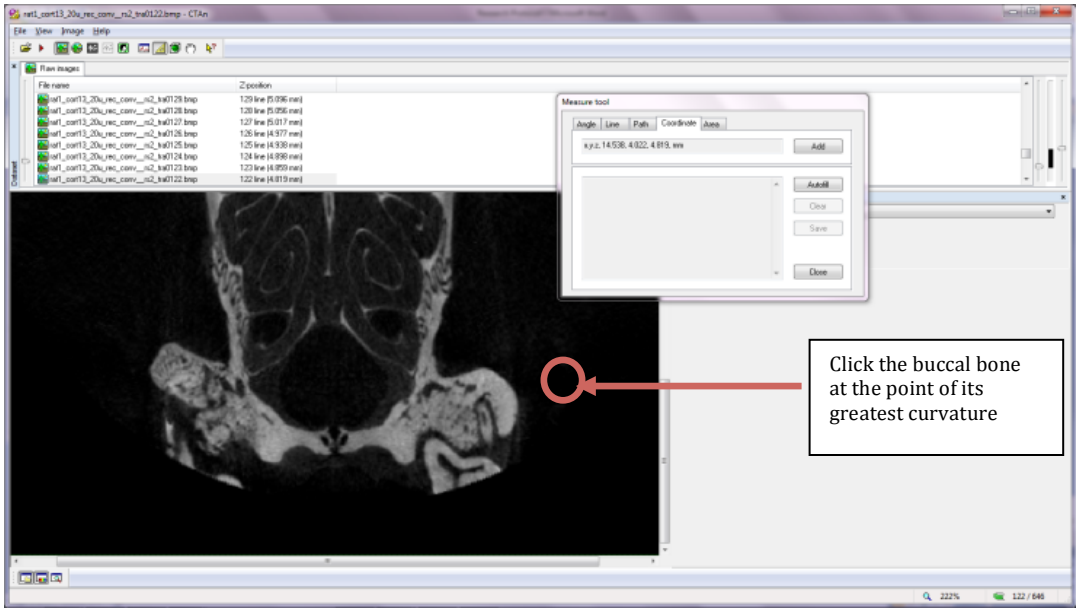

17. Click **Add** in the **Measure Tool** window. The coordinates are now saved in the lower box of the Measure Tool window. This coordinate served as the **buccal limit** when drawing the **region of interest** (ROI). As the buccal bone is variable throughout the slices, the buccal limit is used as a way of standardizing the ROIs between slices. Click **Save** and save the coordinates to a location you prefer. Click **Close** on the Measure Tool window.

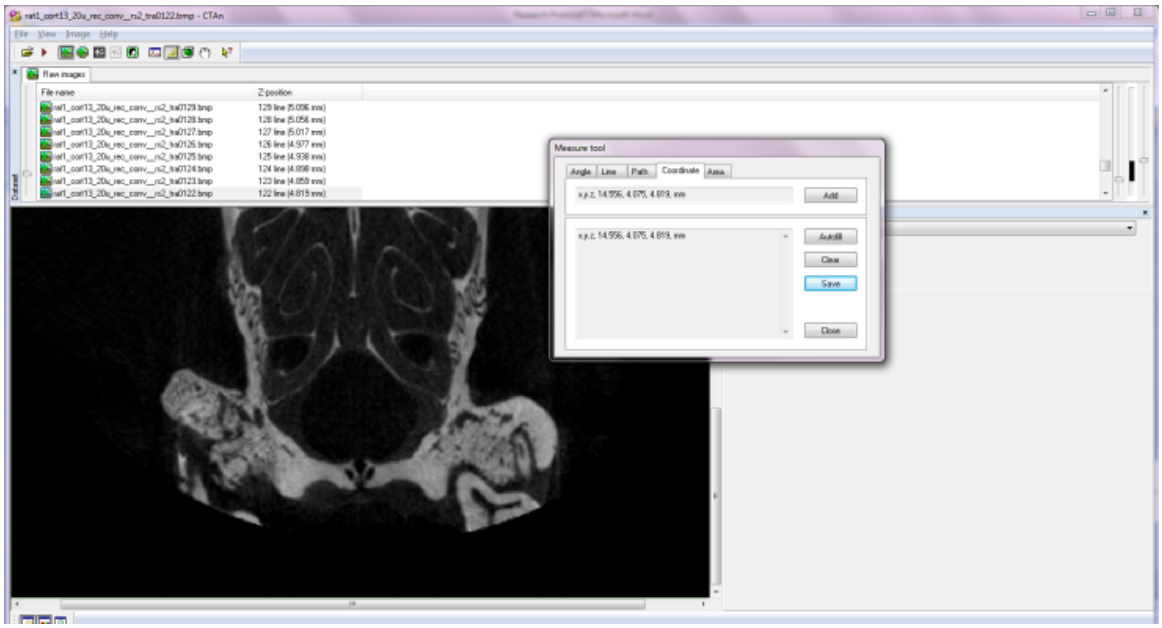

18. Next, the ROI is drawn. The ROI refers to the area of the image that will undergo MicroCT analysis. In this case, the alveolar bone of the first molar is analyzed. When drawing the ROI, the alveolar bone is included and the molar roots and crown are excluded. It is determined that this process cannot be automated and the drawing of ROIs needs to be performed manually. Once the mouse is clicked to begin drawing, the mouse needs to remain depressed until the ROI is completed. The buccal coordinate previously saved is the **buccal limit** and the midpalatal suture is the **lingual limit**.

19. To begin drawing the ROI, switch to the coordinate view by clicking on the **coordinate tab** and selecting the **measure tool**. Click the slice at the **buccal limit**. The Measure Tool shows exact coordinates of the selected point. Re-select the point on buccal bone until the buccal limit coordinates exactly match the coordinates previously determined. The first two numbers of the coordinates needed to match.

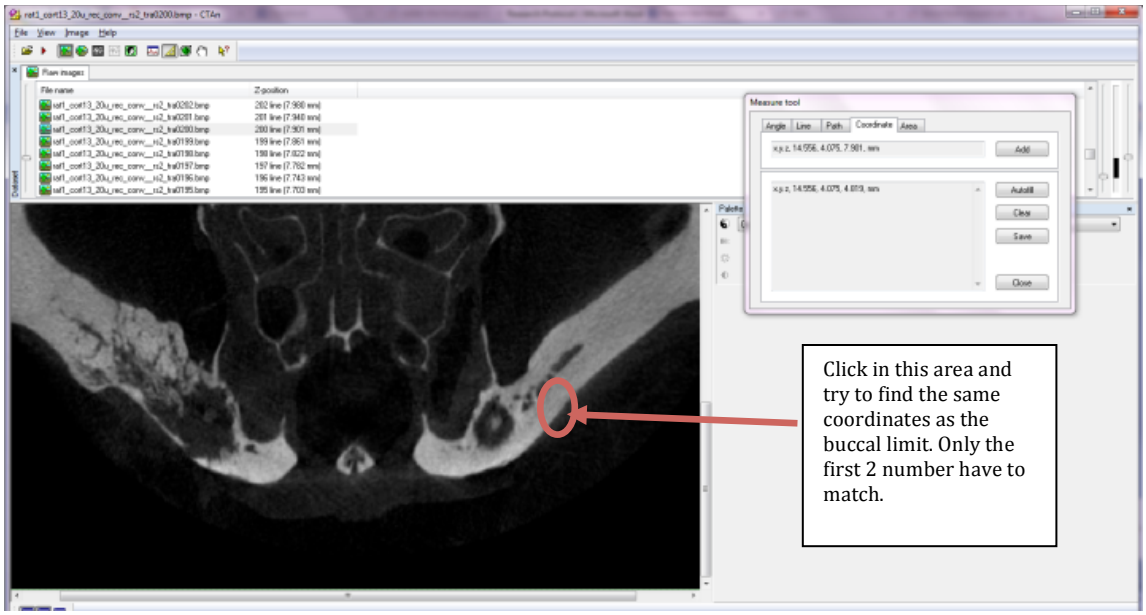

20. Without moving the cursor, press the **ALT** key. Click the **right arrow key** until the **Image tab** is selected. Then, click the **down arrow key** until **Measure** is selected followed by **Enter**. The Measure Tool window should disappear.

21. Without moving the cursor, select **ALT +2** . This keyboard shortcut displays the **Region of Interest (ROI)** tab. The image now appears red. The ROI is ready to be drawn. Since the cursor had not been moved, this ROI drawing begins at the buccal coordinate.

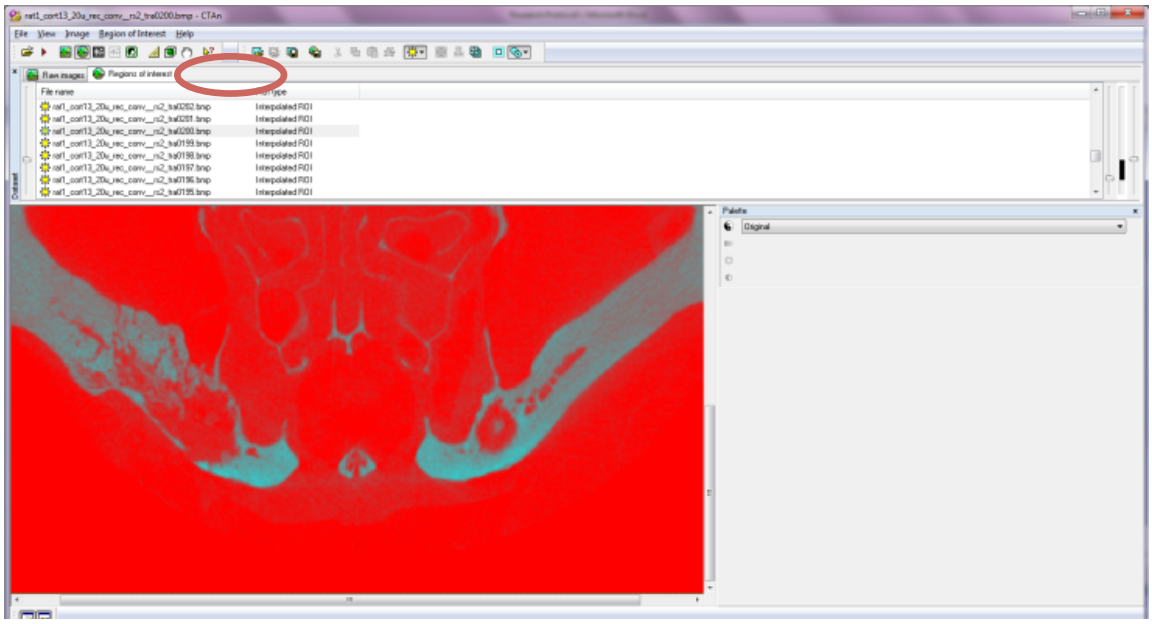

22. Depress the left click on the mouse/trackpad to begin drawing the ROI. Starting at the buccal limit, draw around the roots in the following order starting with the 1) crestal bone, 2) the midpalatal suture (medial limit), and then loop back around to end up back at the buccal limit. Once the loop is completed, the ROI appears. The **Red Shaded** area indicates soft tissue/PDL/empty space. The **Blue Shaded** area is bone.

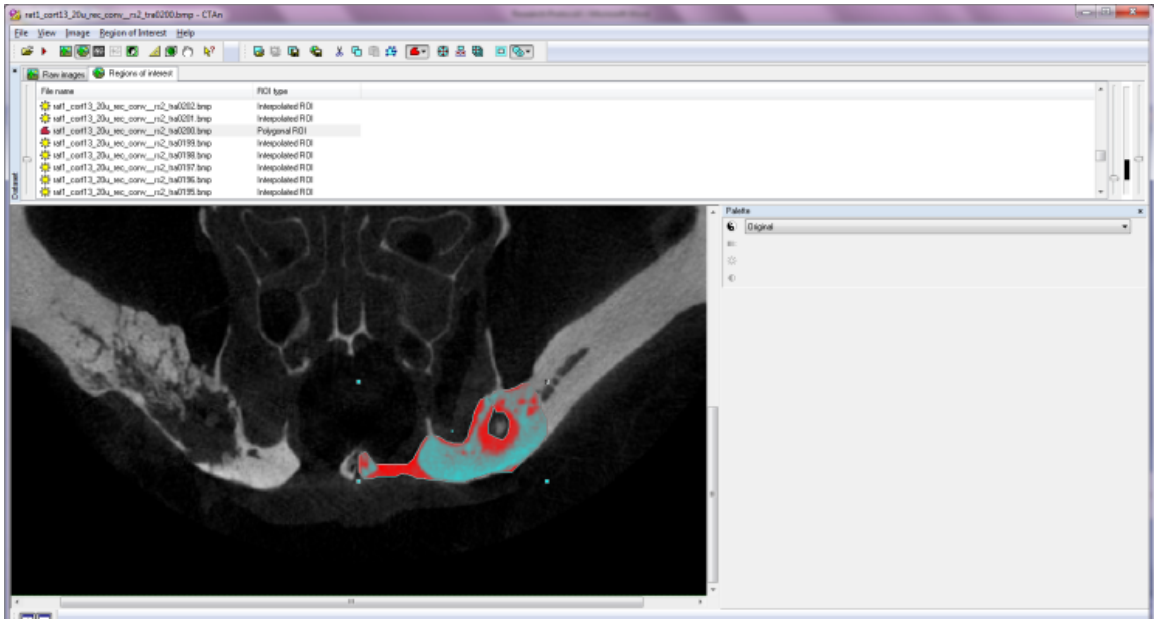

23. Scroll through the images in the **Region of Interest** tab. None of the ROIs should include the tooth. If the ROI starts to include tooth structure or the ROI fails to adapt to the changing bone, draw another ROI for that image. Repeat steps 19-22 to ensure that the ROI drawing begins at the **Buccal Limit**. Repeat this process about every 7th slice until the **Distal Limit** is reached. Draw approximately 16 ROIs for each side per sample to ensure an accurate analysis of the bone.

24. After all of the ROIs are drawn, click the **Binary Selection Icon**. The ROI will appear black and white, while the rest of the non-analyzed image appears green. The black refers to empty space/PDL/soft tissue while the white is hard tissue (bone/tooth). Once again, verify all ROIs to ensure that no tooth structure is included, which appears white. If needed, return to the Region of Interest Tab to redraw the ROIs.

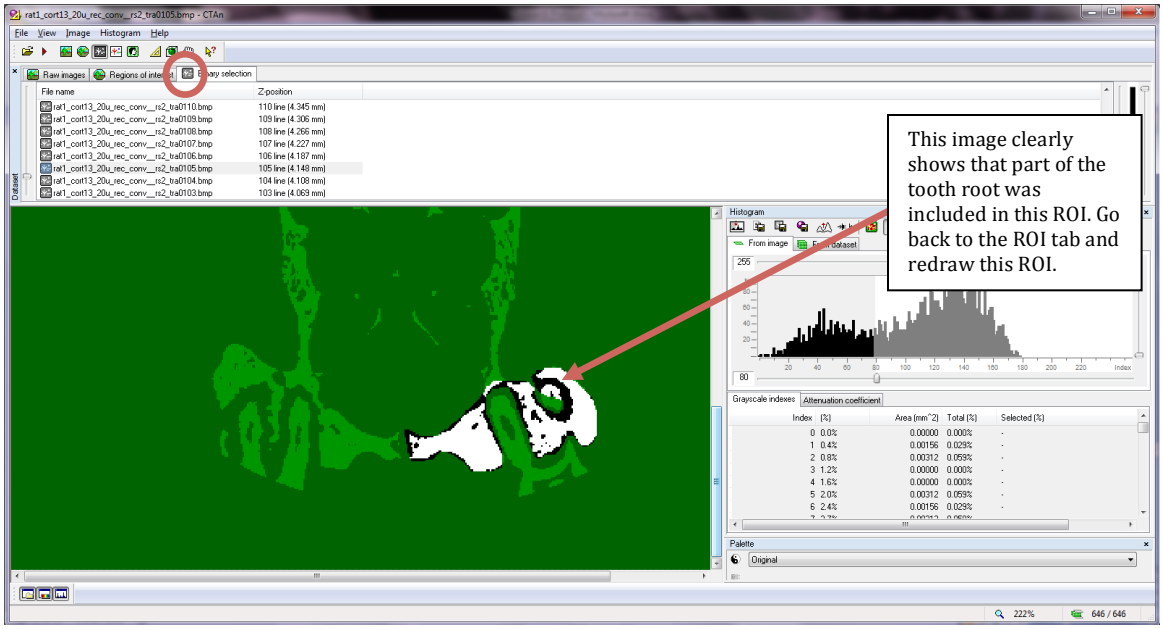

25. To Redraw a ROI, return to the **Region of Interest** tab. Scroll to the image that has an incorrectly drawn ROI. Click the **Cut** icon to remove the ROI. Repeat steps 19-22 to redraw the ROI correctly.

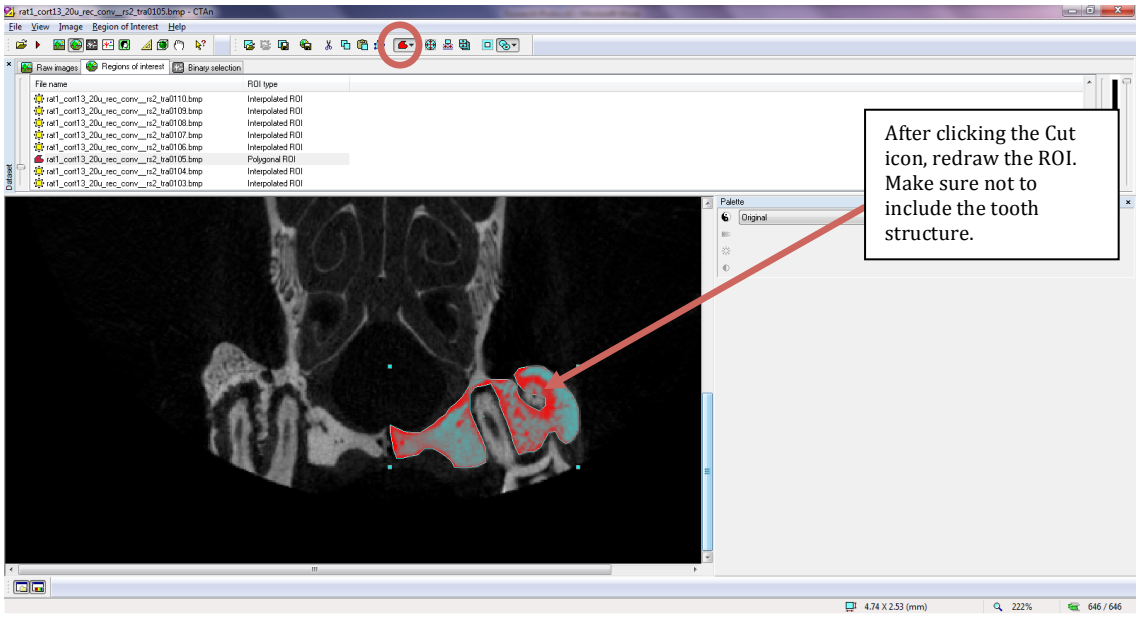

26. Once the ROIs are satisfactory, click back to the **Binary Selection** Tab. Click **File**, then click **Preferences**. Select the **Histogram** tab and make sure the values in the equation are **252.945** in the upper box and **4366.11767** in the lower box, then click OK. These are BMD values for two phantom rods that were previously established.

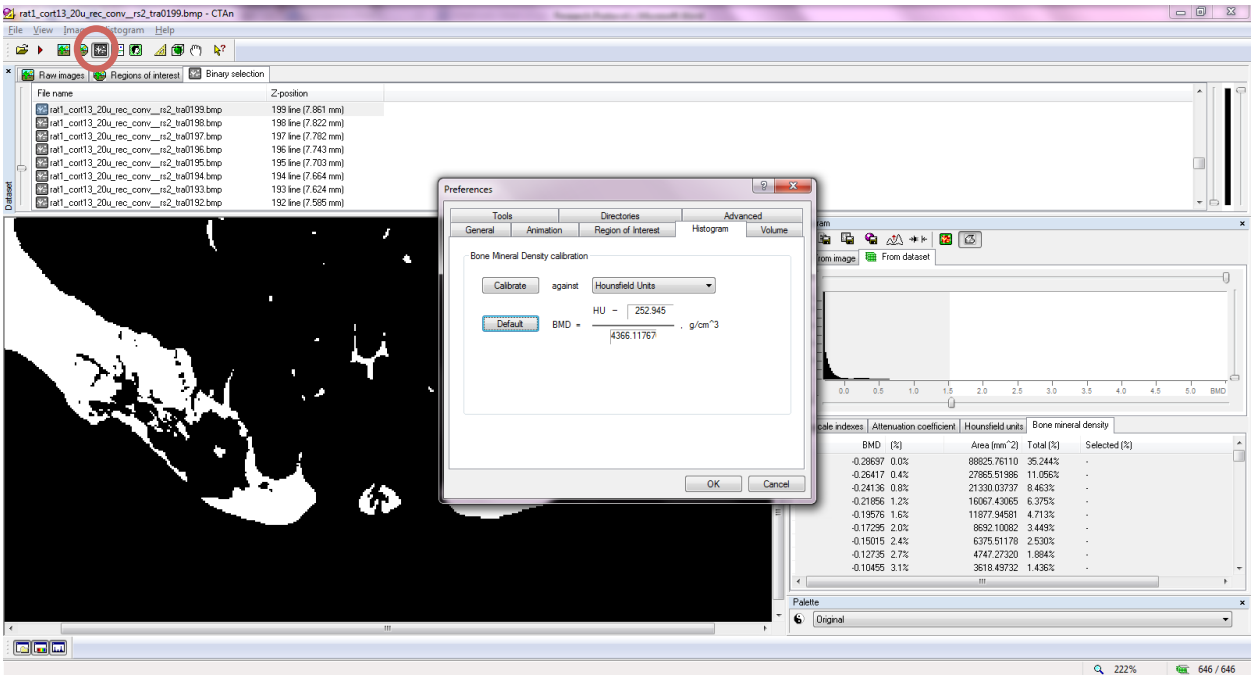

27. Click the **From Dataset** tab. Make sure the values are **255** in the upper box and **80** in the lower box. These are the range of greyscale units for bone, with 80 representing the lower limit and 255 representing the upper limit for the brightness spectrum. The maximum grey level of 255 corresponds to Hounsfield units of 24388. The Hounsfield scale is a quantitative scale for describing radiodensity. Then click the **Density Range Calibration** icon.

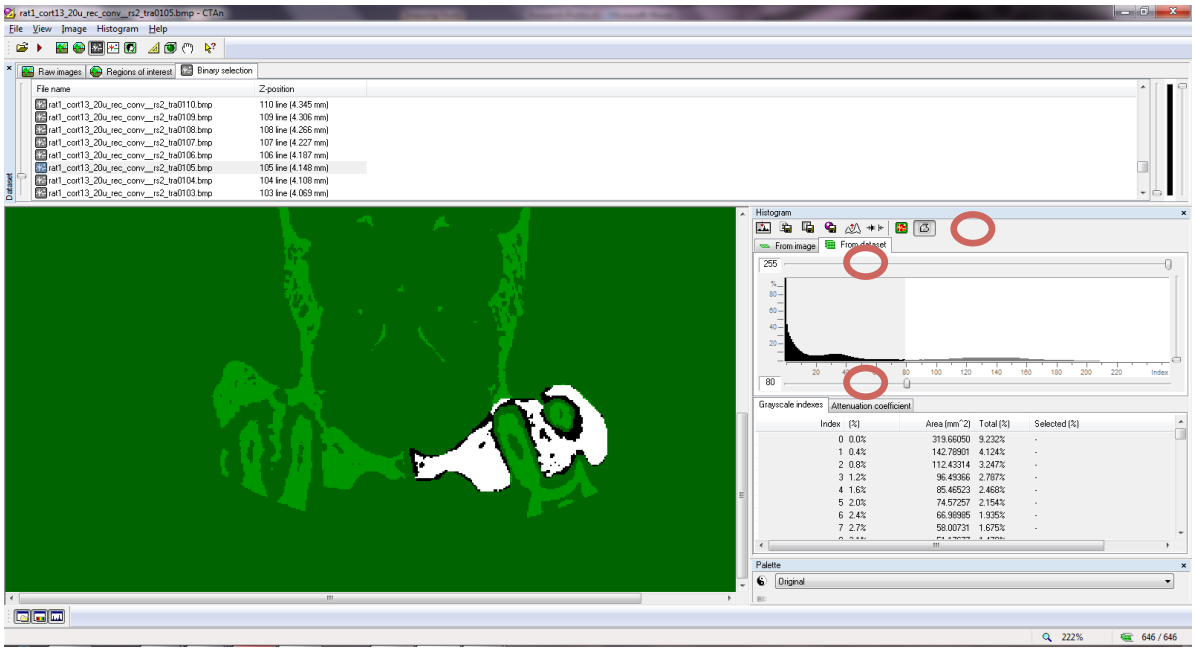

28. The **Density Range Calibration** window appears. In the Upper Right box, type in **10.04424**, which is the grey value for water. In the Lower Left box type **-1000**, which is the Hounsfield units that corresponds to 0 grey level, or air. Click OK.

29. After clicking OK, the **Hounsfield Units** tab and the **Bone Mineral Density** tab should now appear.

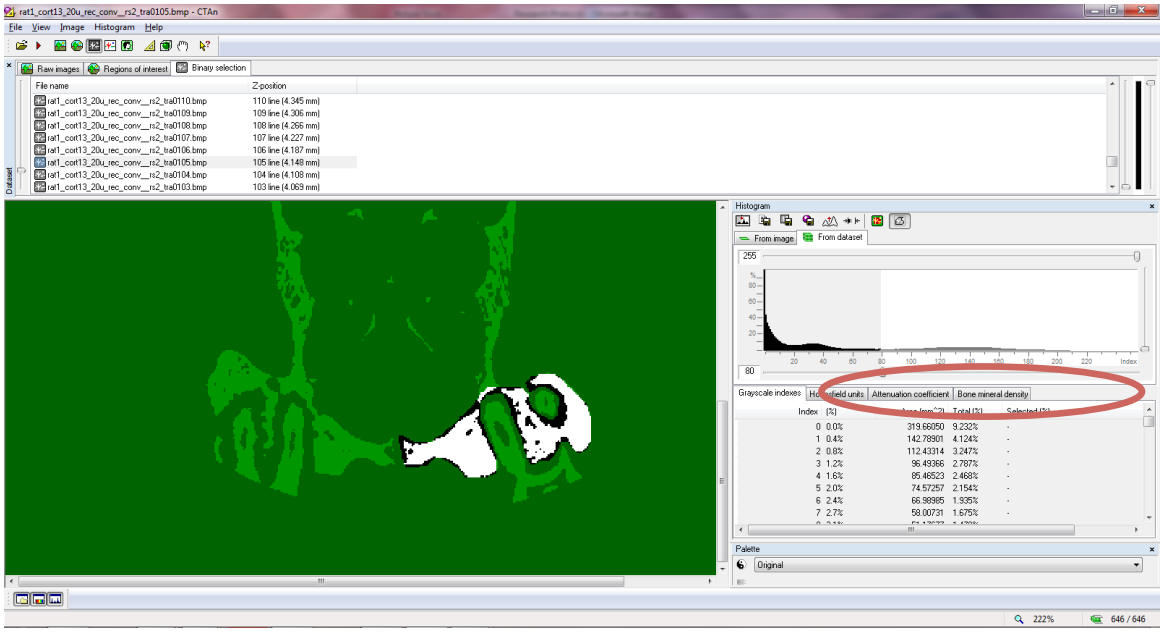

30. Click the **Bone Mineral Density** Tab. The bone mineral density (BMD) is a measurement of the density of minerals in the bone surrounding the first molar of the rat. The value is measured in gram / cm 3. Click the **Save Histogram** icon and save the data to a preferred location.

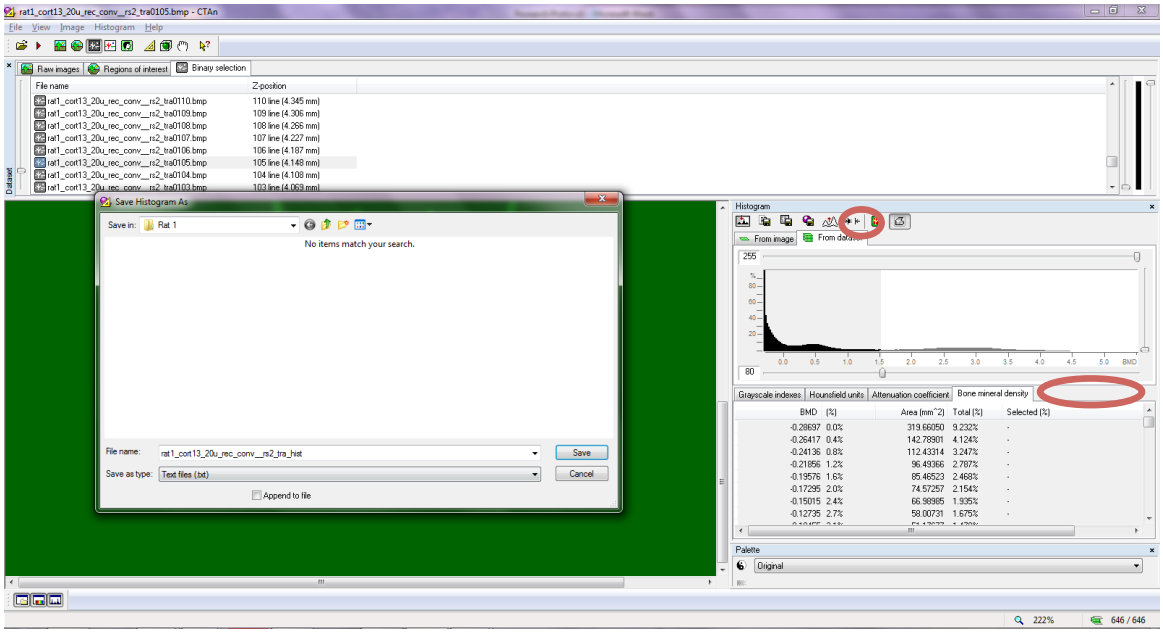

31. Click the **Morphometry** icon. The Morphometry tab will appear. The bone will appear grey. Everything else has been excluded in the image.

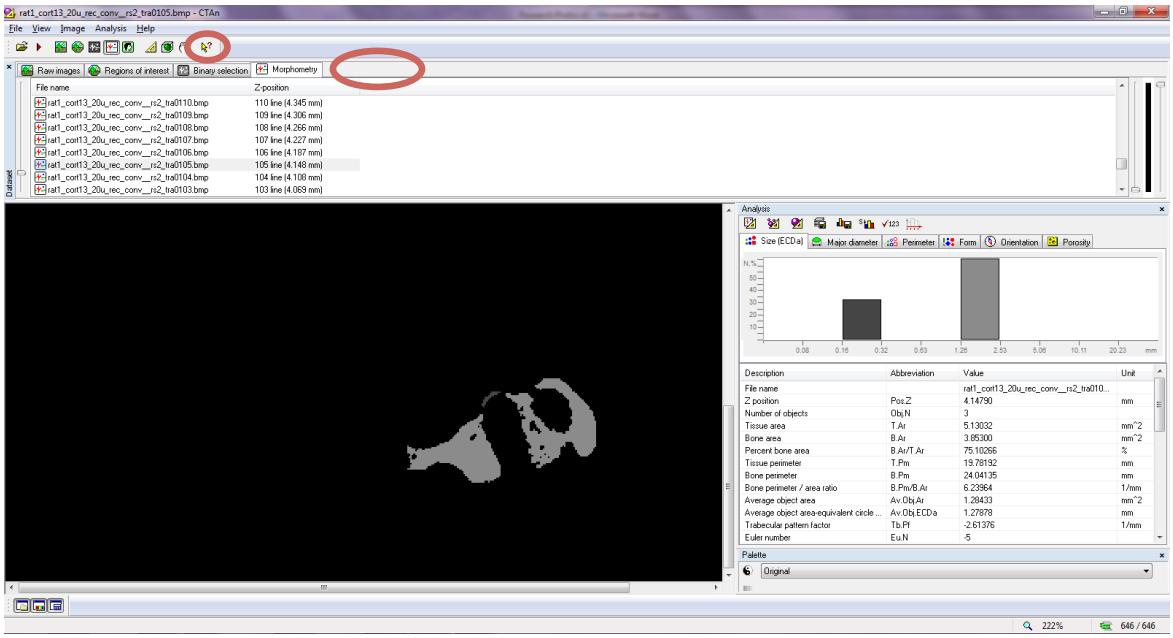

32. Click the **3D analysis icon**. The **3D Analysis** window will appear. Click **continue**.

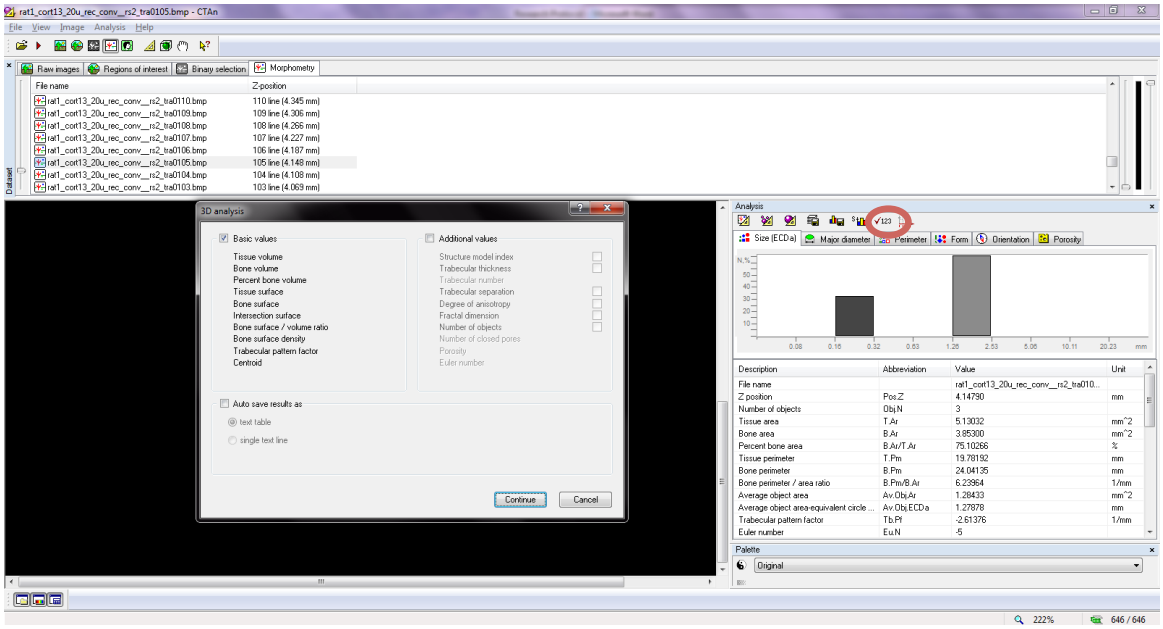

33. A new **3D analysis results window** will appear. The CTAn software calculates the Bone Volume (**BV**) and Percent Bone Volume (**BV/TV**) based on the drawn ROIs and the samples. BV is measured in mm^3. It is the amount of space surrounding the first molar that is occupied by mineralized bone. Bone fraction (BV/TV) is measured as a percentage. This percentage is the amount of bone (BV) compared to the total volume (TV) surrounding the first molar of your sample. Click **Save Results** and save the data to a preferred location.

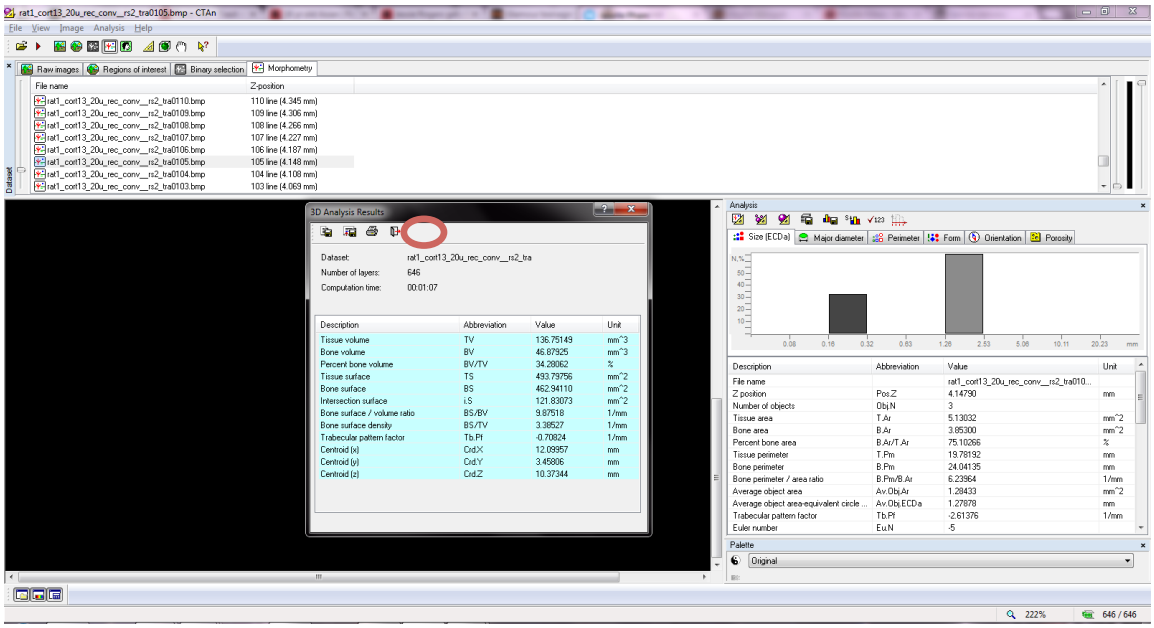

34. Click back to the **Region of Interest** tab. Click the **Save ROI** icon and save the ROI to the preferred location. Previously saved ROIs can be reloaded by clicking the **Load ROI** icon.

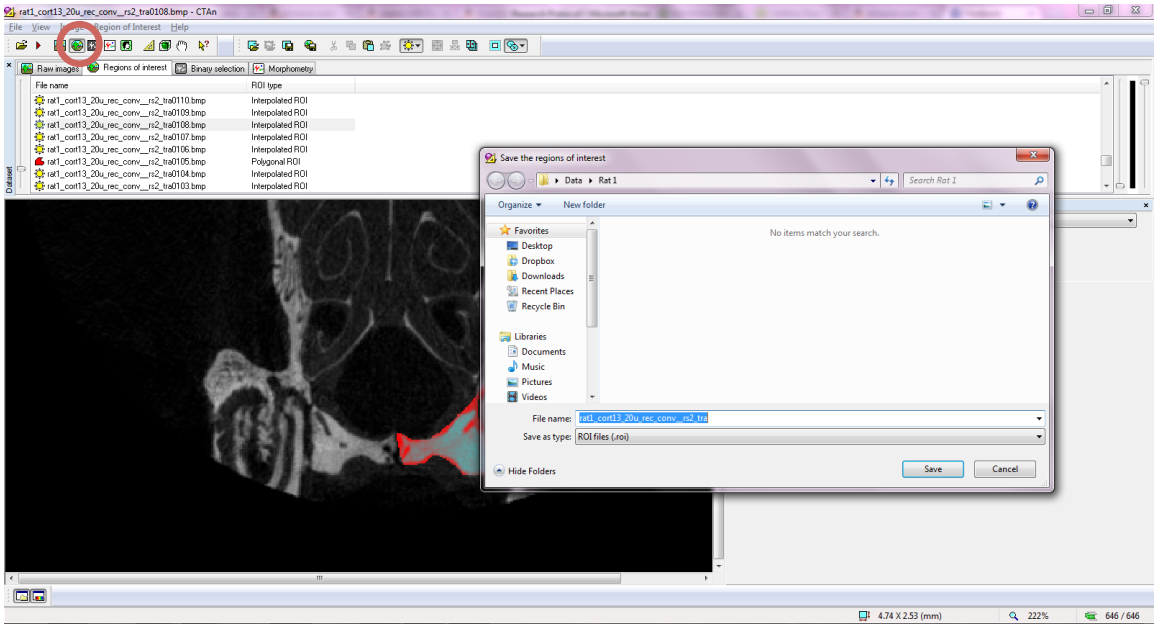

C6: Histological Analysis:

Samples were decalcified in 14% neutral buffered EDTA for 21 days, embedded in paraffin and grossed for H&E staining for qualitative analysis followed by TRAP staining for osteoclast quantification. Three serial slices per section (CA and CR) subjected to TRAP staining. The following is modified version of the Sigma Aldrich TRAP protocol:

1. Pre-heated a 10 mL of DI water to 37° C.
2. De-paraffinized slides at 60° C for about 30 minutes or until the slides were clean
3. Rehydrated the slides in:
    a. 2x Xylene (5 min each)
    b. 2x 100% EtOH (1 min each)
    c. 2x 95% EtOH (1 min each)
    d. 1x 70% EtOH (1 min)
4. Rinsed slides in tap water 3x
5. Prepared TRAP staining solution per the table below:

	5 mL	9 mL
Fast Garnet GBC Base Solution	50 uL	100 uL
Sodium Nitrate Solution	50 uL	100 uL
Mix gently for 30 sec. let stand for 2 min		
Warm ddH_2O (~37°C)	4.5 mL	9 mL
Naphthol AS-BI phosphate solution	50 uL	100 uL
Acetate Solution	200 uL	400 uL
Tartrate Solution	100 uL	200 uL

6. TRAP solution added to slides.
7. Slides placed in humidity chambers then incubate in 37° C for 1 hour. Concealed chambers in foil to prevent light exposure.
8. Verified staining under microscope at 100X magnification before proceeding to the next step. The osteoclasts should appear red.
9. Rinsed with tap water 3X
10. Counterstained with hematoxylin solution for 8 seconds. Rinse with tap water. Verify counterstain under microscope at 100X magnification before proceeding to the next step. Osteoclasts should appear purple
11. Mounted slides using aqueous mounting solution.

Osteoclasts were counted under 100X magnification. When it was unclear whether a cell was an osteoclast or not (black arrows), the area of interested was evaluated at 200X or 400X magnification (**fig. 4**)

D. RESULTS

D1: Statistical Analysis

Paired T-Tests were used to establish significance, which is the standard test for within subject design. Rat 2 was excluded as there was iatrogenic exposure of the pulp from a retention groove that was cut too deep (**Fig. 5**). This trauma resulted in bone infection and excessive bone loss.

D2: In-vivo Measurements

Intra-oral diastema measurements with a digital caliper were taken on Day 0 and Day 21 for each of the six animals. Measurements were taken from the cementoenamel junction (CEJ)

on the mesial side of the maxillary first molar to the CEJ of the lingual side of the maxillary incisor. **Fig. 6a** depicts the change in diastema length between Day 0 and Day 21, showing a greater change in the corticotomy group. **Fig. 6b** depicts the average change in diastema between Day 0 and Day 21, which showed a 30% increase in tooth movement on the corticotomy side. During the experimental period, two of the appliances were dislodged. However, the duration without the appliance was limited to less than a day, as rats were checked on a daily basis to assess if any appliances needed to be resecured.

D3: MicroCT Analysis

Post-sacrifice, all animals were subjected to microCT analysis to evaluate the condition of the corticotomies, and calculate bone fraction (BV/TV) and bone mineral density (BMD). MicroCT analysis of training rat (separate from the experimental animals) that was sacrificed on Day 7 showed that the corticotomies were still visible. The rats in the experimental group that were sacrificed on Day 21 showed healing of corticotomies (**Fig. 7**).

The corticotomy side showed greater BV/TV when compared to the control side in all animals (**Fig. 8a**). On average, the corticotomy side showed 7% greater bone fraction on Day 21 compared to the control side (**Fig. 8b**). The corticotomy side showed greater BMD than then control side (**Fig. 9a**). On average the corticotomy side showed 10% increase in BMD compared to the control side on Day 21 (**Fig. 9b**).

D4: Histological Analysis

Histomorphometric analysis with H&E allowed for evaluation of bone quality, root resorption, and presence of inflammation. Osteoclasts could be visualized but were not quantifiable with H&E staining. Examination of the slides showed that the corticotomy side revealed greater root resorption (**Fig. 10a**) when compared to the control side (**Fig. 10b**). The

corticotomy side also revealed greater presence of new bone formation (**Fig. 11**). New bone formation was quantified on H&E by defining a fixed size rectangle for the right and left sides that enclosed the alveolar bone of the first molar for each rat. The areas of new bone were measured and the percent new bone formation was calculated using the following equation: Σ new bone area / total alveolar bone area. The corticotomy side in each rat showed between 3% to 6% greater new bone formation compared with the corticotomy side (**Fig. 12**).

Although osteoclasts were visualized using H&E staining, the quantity of osteoclasts was confirmed with TRAP staining. The corticotomy side showed a greater number of osteoclasts than the control side across all animals in the alveolar bone and intraradicular bone (**Fig. 13a**) and on the pressure side bone (**Fig. 14a**). There were 44% more osteoclasts in the alveolar and intraradicular bone of the corticotomy side compared with the control side (**Fig. 13b**). There were 55% more osteoclasts in the pressure side bone of the corticotomy side compared with the control side (**Fig. 14b**).

E: DISCUSSION

The rate of tooth movement during orthodontic treatment depends on the interplay of bone remodeling activities and the rates at which these activities occur. The dynamic process of bone resoprtion and formation allows the tooth movement to occur. Presumably, decortication promotes alveolar bone turnover and RAP occurs. Although there have been several studies on corticotomy assisted tooth movement, this is the first that utilizes the orthodontic mini-implant driver to pierce through the gingiva with subsequent decortication of the alveolar bone in rats. In other rat studies, Teixeira et al. (2009) raised soft tissue flaps and decorticated the bone with a ¼ round bur affixed to a high speed handpiece (56) and Baloul et al. (2011) similarly raised a flap prior to placing corticotomies with a ¼ round bur affixed to a low speed handpiece (5). In both

instances, periodontal surgery occurred prior decortication. Our study avoids periodontal surgery and utilizes the mini impl ant driver, which may achieve higher patient acceptance as patients do not need to undergo periodontal surgery first, and the decortication will be performed more gently with a manual implant driver. The current techniques utilizing mechanical trauma to decorticate are more aggressive than our proposed technique: 1) Wilckodontics involves raising a flap followed with decortication with a bur (62), 2) corticision and mallet involves driving a knife through the gingiva and cortical bone with the assistance of hammer (44), 3) piezocision involves cuts with a vibrating knife (13) and 4) piezopuncture utilizes a vibrating endodontic condenser (32). Although these four modern techniques are effective at inducing RAP and subsequent ATM, they may lack patient acceptance due to their invasiveness. Although a similar appliance to the mini implant has been produced, marketed and tested in humans only (2), this tool is non-autoclavable and is disposable. It would be more practical for the orthodontist to use a device that is already part of the basic armamentarium that does not require water or saline cooling mechanism and can be sterilized.

Our study was also the first of its kind to utilize a split mouth design with corticotomy and orthodontic tooth movement on one side of the maxilla versus orthodontic tooth movement alone on the contralateral side using the first molar and incisor as anchorage units. It can be surmised that other studies chose not to use a split mouth design because of the difficulty in placing bulky orthodontic appliances in the rat oral cavity, which is very small. Perhaps there was concern that the RAP effect subsequent to corticotomy on one side would migrate over to the contralateral side. However, split mouth studies are considered the optimal conditions for studying a treatment effect on tooth movement, as they maximize statistical power within a fixed number of observations (39). A previous study utilized a split mouth design, except that the

anchor units were the opposing second molars (24), and therefore lacked a "fixed" or absolute anchor unit. The split mouth design allowed us to control for inter-animal differences and also reduce the costs of the study. Furthermore, other rat studies enhanced the security of the orthodontic appliance by either 1) drilling a hole through the alveolar bone of the maxillary incisor (49) and then threading a ligature through this hole, 2) drilling a hole laterally through the incisors and ligating through this hole (30, 56, 64), or 3) placing an implant in this region (5, 14), and using the implant as an anchor. Although these methods are more secure, there is also the risk of additional inflammation from alveolar bone injury or pulpal trauma, which would be confounding factors in the study. Our study demonstrated that injury to the pulp in one animal resulted in severe bone infection and destruction, and consequently this animal showed decreased values for BV/TV and BMD compared with the other animals. We devised a retentive yet non-destructive method to secure our appliance: a groove placed on the facial aspect of the incisor, along the cemento-enamel junction served as a pit to secure the steel ligature. As our technique did not prevent the incisors from erupting as a mini implant anchor would have, the appliances needed to be checked on a daily basis and re-secured as needed. Other studies secured the appliance in a similar manner (14, 54, 61), however, a split mouth appliance design was not utilized and how the appliance would be re-secured as a consequence of continuous incisor eruption was not always addressed.

The change in diastema measurement between day 0 and day 21 when comparing corticotomy side versus control side demonstrated that 30% greater tooth movement occurred on the corticotomy side. A previous study using a digital caliper to assess the amount of tooth movement in-vivo supports the finding of increased tooth movement on the corticotomy side (5). The molar on the corticotomy side was able to move a greater distance because the bone on the

pressure side had been demineralized with corticotomy, which decreased the resistance to movement(36)

MicroCT analysis on Day 21 revealed a 7% and 10% increase in BV/TV and BMD, respectively, on the corticotomy side compared with the control side with the exception of the excluded animal (rat 2). Rat 2 demonstrated decreased BV/TV and decreased BMD at 21 days. This anomalous finding is most likely attributed to the retention groove placement that resulted in pulp exposure and subsequent bone infection and destruction. This infection likely resulted in impaired anabolic bone activity and subsequently reduced ability of the animal to recover normally from the initial osteopenic effect of corticotomy. Bone healing after injury involves a cascade of complex intracellular and extracellular events that remains to be fully elucidated. A genetic alteration in BMPs or any of the other essential signaling molecules could cause a healing delay (15). The other animals showed increased BV/TV and BMD 21 days after corticotomy. Bone remodeling occurs in response to forces applied to teeth. Bogoch et al. (1993) found that there was a fivefold increase in bone formation in the adjacent bone following osteotomy, suggesting that RAP occurs regardless of whether the surgical procedure was an osteotomy or corticotomy (6). An increase in BV/TV and BMD in the corticotomy side could be attributed to corticotomy stimulating bone anabolic activity. Baloul et al. (2011) showed that BV/TV and BMD were increased in the corticotomy plus tooth movement group compared to the tooth movement group alone at 28 days. The corticotomy group alone showed the greatest BV/TV and BMD at 28 days compared with corticotomy + tooth movement and tooth movement alone groups (5).

H&E showed between 3% to 6% increased new bone formation in the aveolar bone on the corticotomy side. Future studies to understand better new bone mineralization in animals

undergoing corticotomy would be to perform intra-vital staining at various time points: 1) Day 0, 2) Day 7 (as the greatest amount of tooth movement occurs in the first week) and 3) Day 21. On H&E for half the samples, moderate root resorption was observed on the corticotomy side. However, there are limitations when evaluating root quality on H&E, as each H&E slide represents one section of the entire sample. Further studies to measure and compared root volume between the control and corticotomy sides using microCT would help to shed light the possibility of root resorption. Certain types of tooth movement, specifically root torque, bodily movement and intrusion, cause teeth to be more prone to apical root resorption. This is particularly applicable to our study, as the center of force application was close to the tooth's center of resistance, and thus, it is possible that bodily movement was favored (33). Additionally, previous studies have shown that orthodontic treatment can influence root resorption considerably, particularly in the presence of heavy and compressive forces (58). In our study, 25 g springs were used to close the space, which is the smallest commercially available closed coil spring on the market and used in other studies (5, 14) and recommended by Ren et al. (2004) in a systematic review of literature concerning tooth movement in rats (49). However, the rat molar is 50X smaller than the human molar (49), so even the force of the lightest springs may be excessive for rats. It is arguable that in light of decortication, which transiently demineralizes the alveolar bone, that the teeth should move more easily through the bone, and therefore experience a decreased likelihood of external apical root resorption. Currently, there is a lack of studies evaluating whether decortication has an effect on root resorption (2). What is known is that odontoclast and osteoclast activation both occur during inflammation, particularly following the release of IL-1, TNF-α and other pro-inflammatory cytokines, and both root and bone resorption have been shown to occur as a consequence (26).

We investigated the presence of osteoclasts as a marker for inflammation and bone resorption.. In our study, we found a 44% and 55% increase in the number of osteoclasts in the total alveolar bone and pressure side, respectively in the corticotomy side compared with the control side ($p = .03$). Teixeira et al. (2010) found that soft tissue flap plus decortication plus tooth movement resulted in the greatest number of osteoclasts on day 28 when compared to soft tissue flap plus tooth movement and tooth movement alone (56). One study quantified the total number of osteoclasts within the total alveolar bone (14) whereas another study quantified the osteoclasts on the pressure side only (56). Although the conventional theory behind the biology of tooth movement stipulates that osteoclast activity is confined to the pressure side, a newer study has also suggested that the periodontium remodels as a continuous unit, and the alveolar bone and PDL should not be divided into compartments, such as "tension side" and "compression side" (24). In a study involving low-energy lasers combined with corticotomy to enhance the rate of tooth movement, it was found that rather than the two treatments having a synergistic effect, dual application of these treatments resulted in a reduced rate of tooth movement (31). The results of this study indicate that a treatment rendered on the pressure side could migrate to the tension side and vice versa.

Osteoclast-osteoblast coupling is regulated by completed interactions of cytokines and growth factors. Cytokines involved with increasing osteoclast activity include cytockines IL-β, TNF-alpha, IL-6, IL-1, growth factors FGF-2 and EGF, and chemokines CCLS2, CCL3, CCL6, CCL7, CCL9 and IL-8 (3). Teixeira et al. (2010) found that 37 of the 92 cytokines were uregulated in the combined tooth movement plus corticotomy group (56). The focus of that study was on cytokine regulation of osteoclastogenesis. Osteoblasts play an equally important role in bone remoldeling. OPG synthesis by osteoblasts downregulate osteoclast activation. Further

studies should investigate whether decortication downregulates OPG synthesis, and thus contribute to an increase in osteoclasts..

In preparation for clinical acceptance, it would be beneficial to test our corticotomy technique in a higher animal species. Alikhani et al. (2013) evaluated the effect of osteoperforations using the PROPEL device in humans and found that tooth movement was accelerated in regions that were decorticated and that there were increased levels of IL-1α, IL1β, CCL3, CCL2, TNF-α, IL6, CCL5 and IL8 in the osteoperforation group. The effect of corticotomy on root resorption was not investigated. A number of dog studies evaluating tooth movement (10) and tooth movement accelerated with varying methods of corticotomy (25, 32, 47, 57) have been published. Dog and bovine bone resemble human bone closest in terms of bone density and fracture stress values (1).

Although other decortication methods have been shown to be effective, patient acceptance of these techniques may be limited due to their invasive and uncomfortable nature. Therefore, it is prudent to devise techniques that are less invasive than the former, but still efficacious. Our study lays the groundwork for the use of a modified mini-implant driver as an effective corticotomy tool for accelerating tooth movement while eliminating the need for concomitant periodontal surgery. Further studies are also needed to establish the quantity of corticotomies needed, the time point at which corticotomies are administered, the duration of treatment effect, and subsequently how frequently corticotomy needs to be administered in order to sustain RAP to maximize accelerated tooth movement. Studies investigating root resorption as a consequence of ATM would also help the clinician to better identify patients who would and would not be good candidates for corticotomy

F: CONCLUSIONS

1. The modified mini implant represents the first corticotomy tool that is readily available in the orthodontist's existing armamentarium, is autoclavable (reusable), is hand-driven, and does not require an external cooling mechanism.
2. This study represents the first split mouth study in rats that involves protraction of the first maxillary molar
3. The molar on the corticotomy side moved 30% more compared with the control side at 21 days
4. BV/TV was 7% greater on the corticotomy side compared with the control side at 21 days
5. BMD was 10% greater on the corticotomy side compared with the control side at 21 days
6. H&E analysis showed increased root resorption on the corticotomy side compared with the control side. H&E also revealed 3% to 6% new bone deposited on the corticotomy side compared with the control side.
7. TRAP staining revealed a 44% increase in osteoclast quantity on the corticotomy side compared with the control side when examining the total alveolar and intraradicular bone of the first molar. TRAP staining revealed a 55% increase in osteoclast quantity on the corticotomy side compared with the control side when examining the pressure side bone only.
8. Perhaps avoid intentional penetration to pulp of the rat dentition and additional bone anchorage devices to prevent incisor eruption when considering appliance design.

H: FIGURES

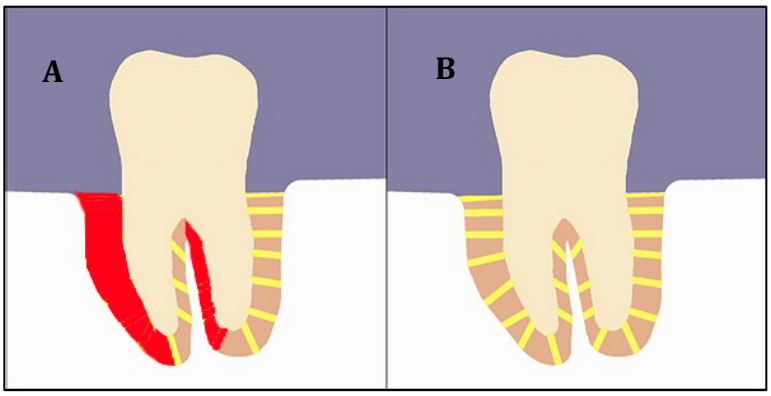

Fig. 1: New Theory of Orthodontic Tooth Movement: Box A shows the currently held theory that bone resorption is limited to areas in red. Box B shows the new theory that the periodontal membrane is 1 communicating compartment.

Fig. 2: Corticotomies Placed in Alveolar Bone: The newly designed tool will place small holes with a mini-implant-like device in the cortex of the alveolar bone.

Fig. 3: Rat with Orthodontic Appliances: Photo depicts split mouth orthodontic appliance placement.

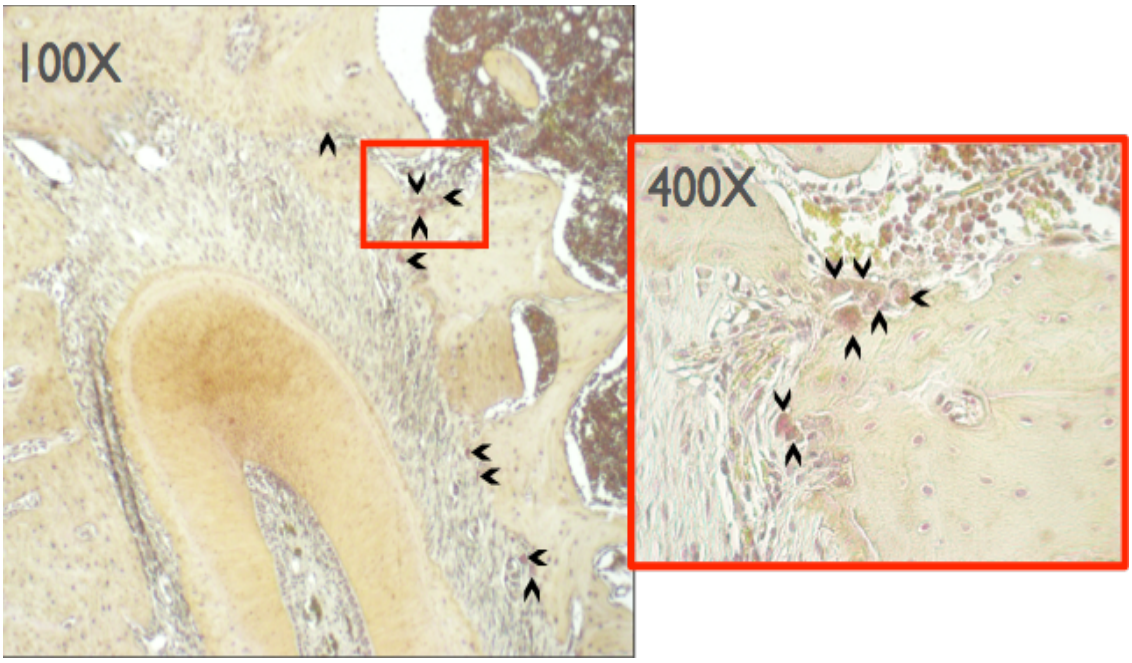

Fig. 4: Osteoclast Quantification: Osteoclasts were routinely counted at 100X, but if further clarification was needed, magnification was increased to 200X or 400X.

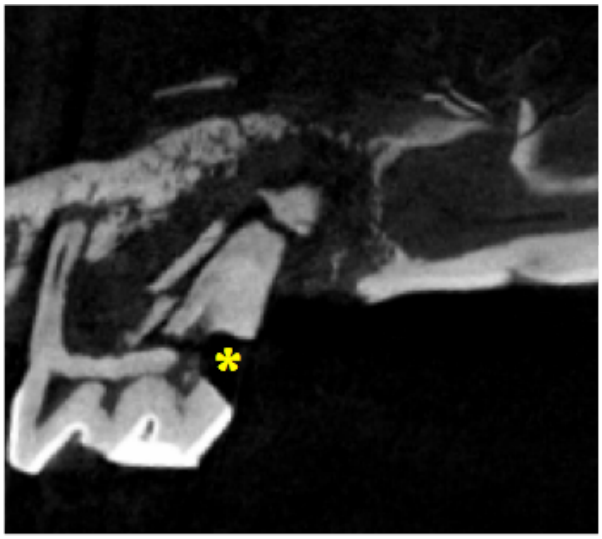

Fig. 5: Iatrogenic Pulp Exposure: Yellow asterisk shows invasion of pulp following placement of retention groove.

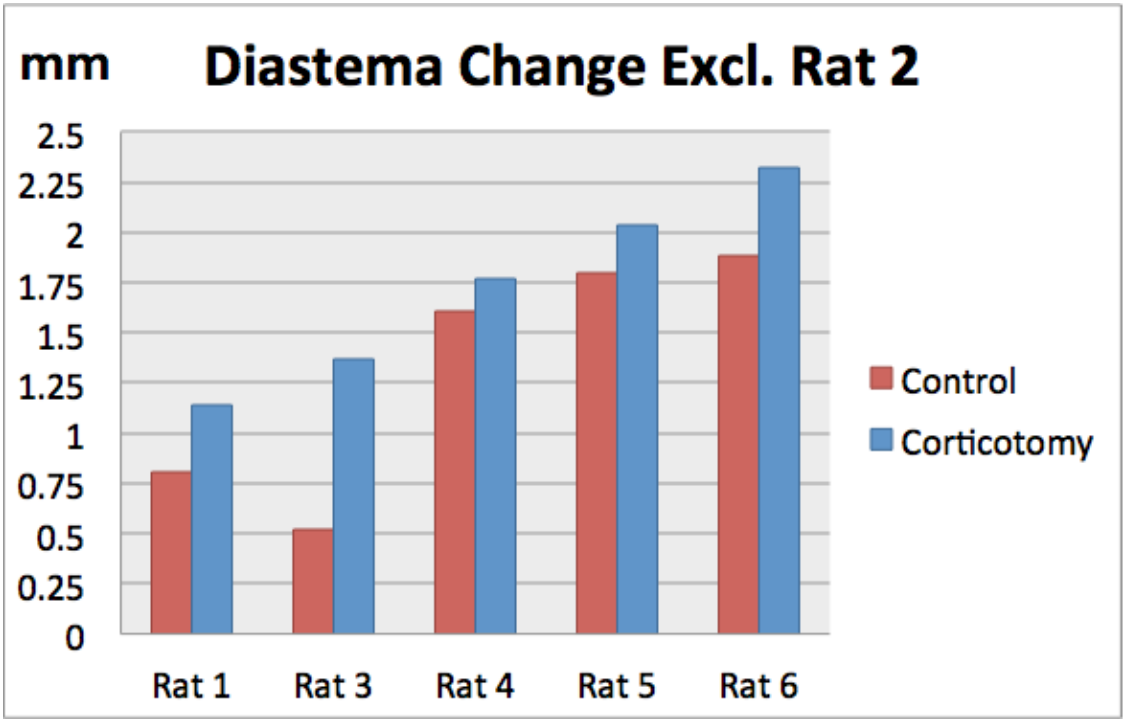

Fig. 6a: Diastema Change: The graph depicts the change in diastema length (mm) from Day 0 to Day 21 for the 5 rats.

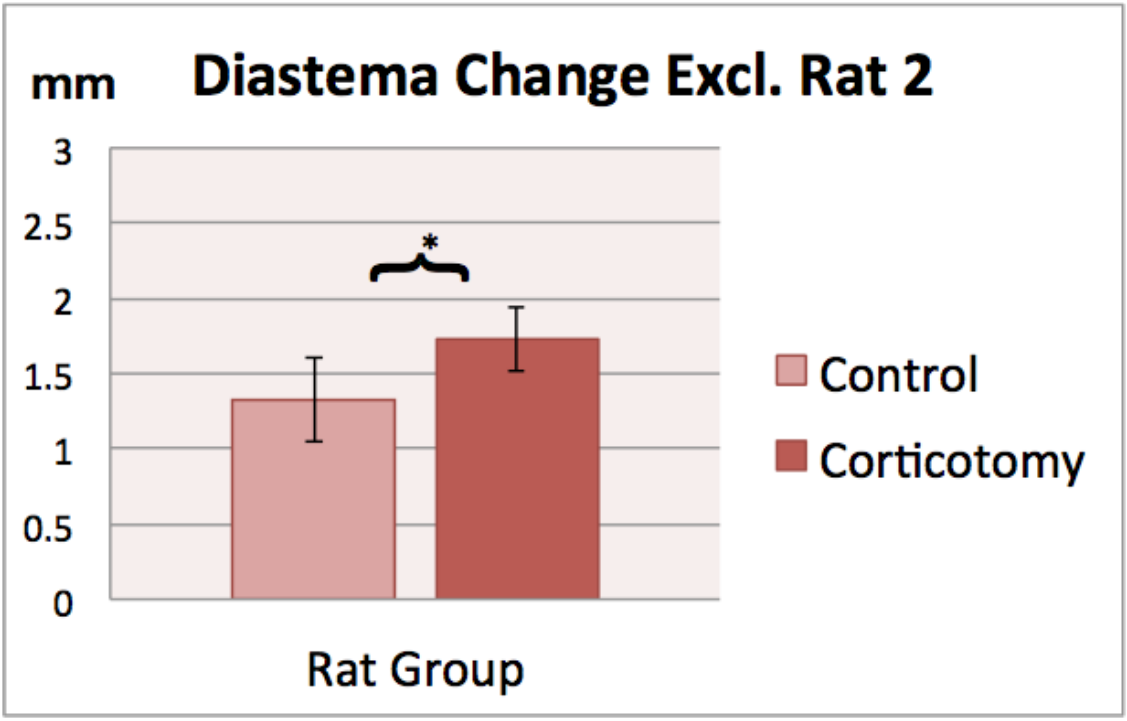

Fig. 6b: Average Diastema Change: The graph depicts the average change in diastema length (mm) from Day 0 to Day 21 for the 5 rats.

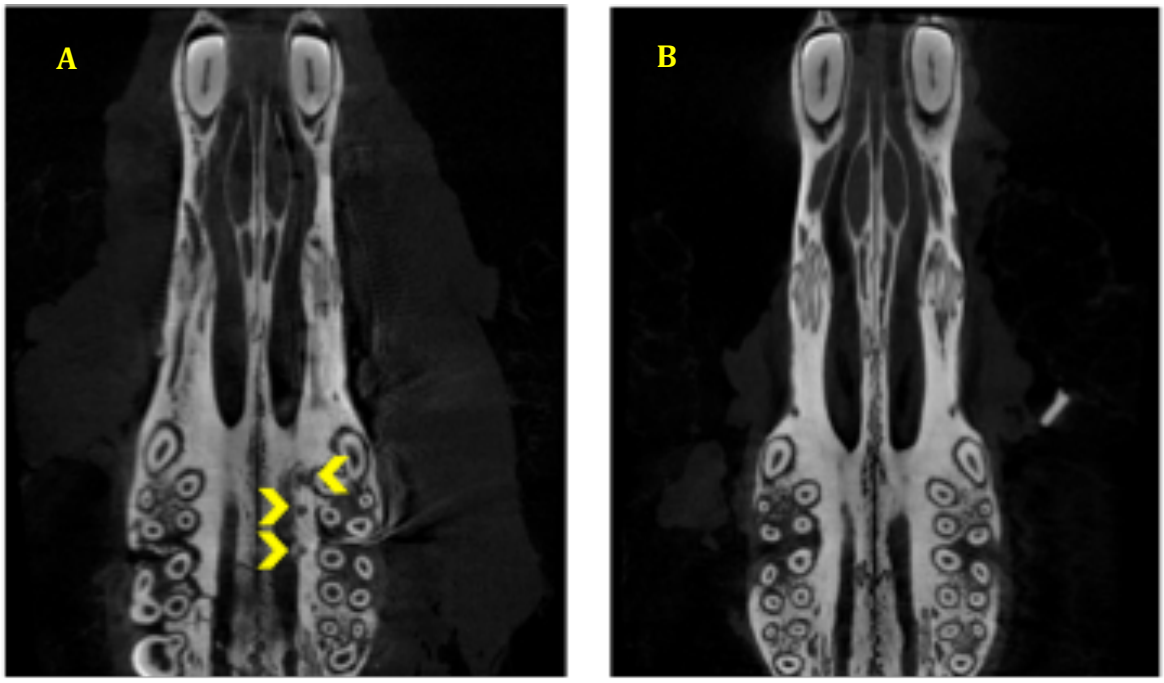

Fig. 7: MicroCT Evaluation of Corticotomies: A) Corticotomies detected at 1-week post treatment (yellow arrows). B) Apparent healing of corticotomies at 3 weeks.

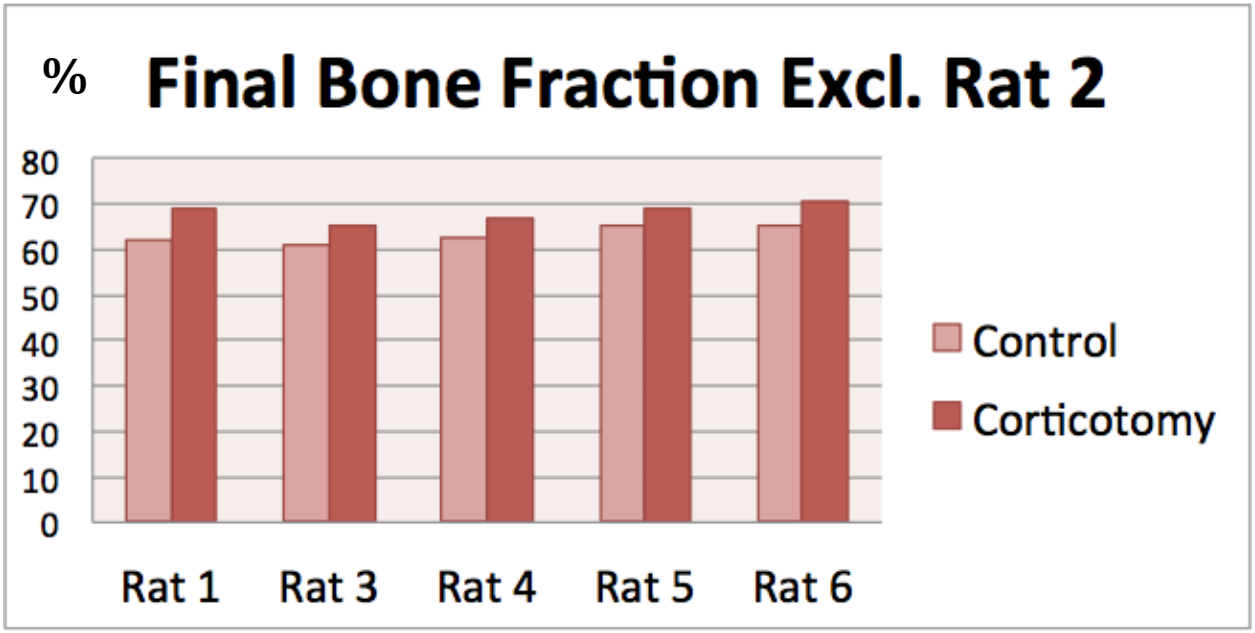

Fig. 8a: BV/TV Analysis: BV/TV comparison between the animals shows that BV/TV was increased in all animals rats on the corticotomy side.

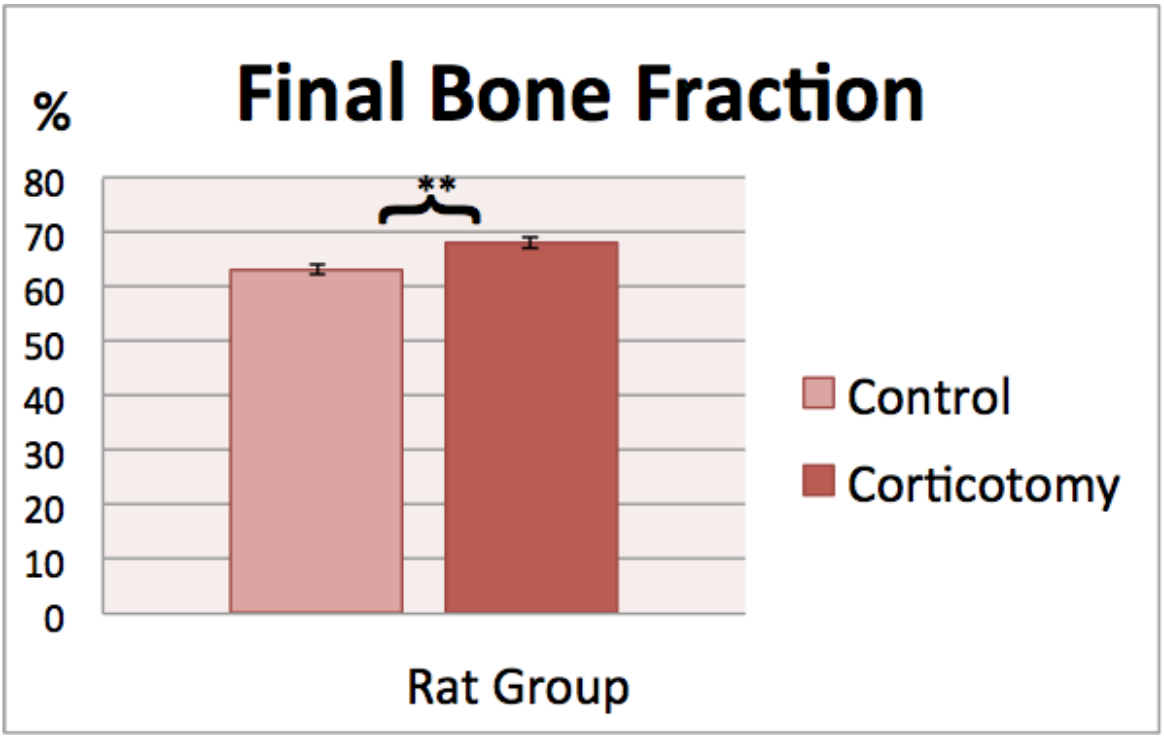

Fig. 8b: Average Results for BV/TV Analysis: BV/TV was 7% greater on the corticotomy side compared with the control side at 21 days. ** $p < .01$

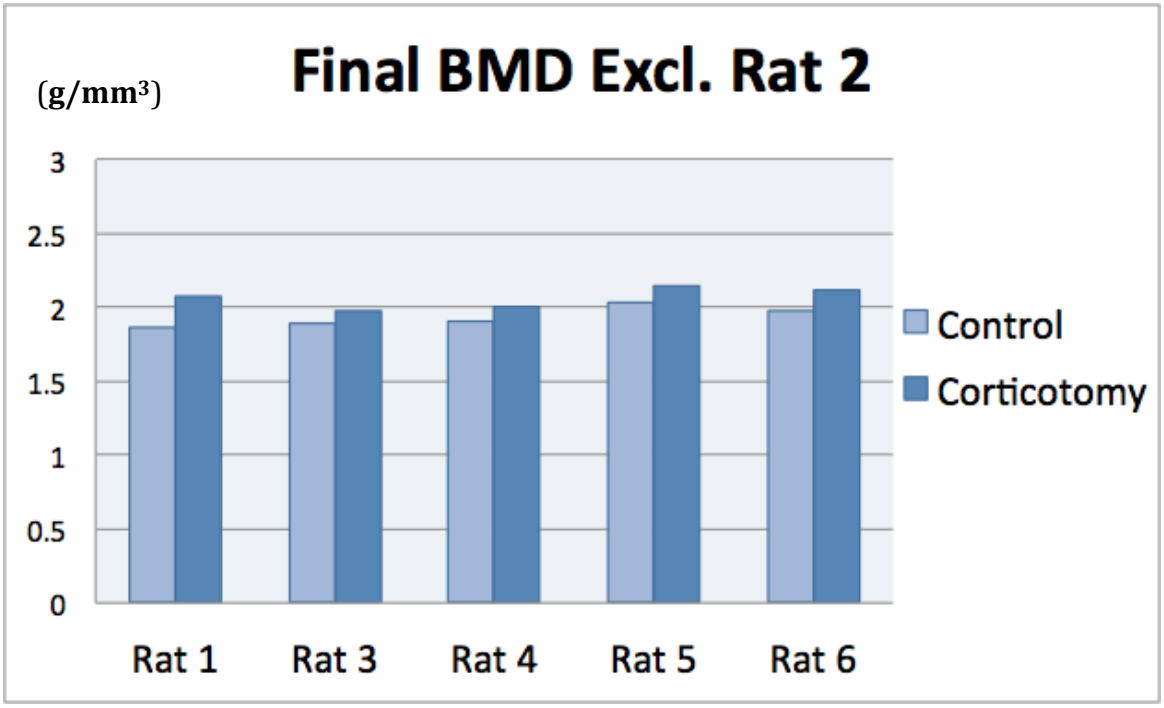

Fig. 9a: BMD Analysis: Excluding rat 2, the corticotomy side on each animal showed greater BMD compared to the control side at 21 days.

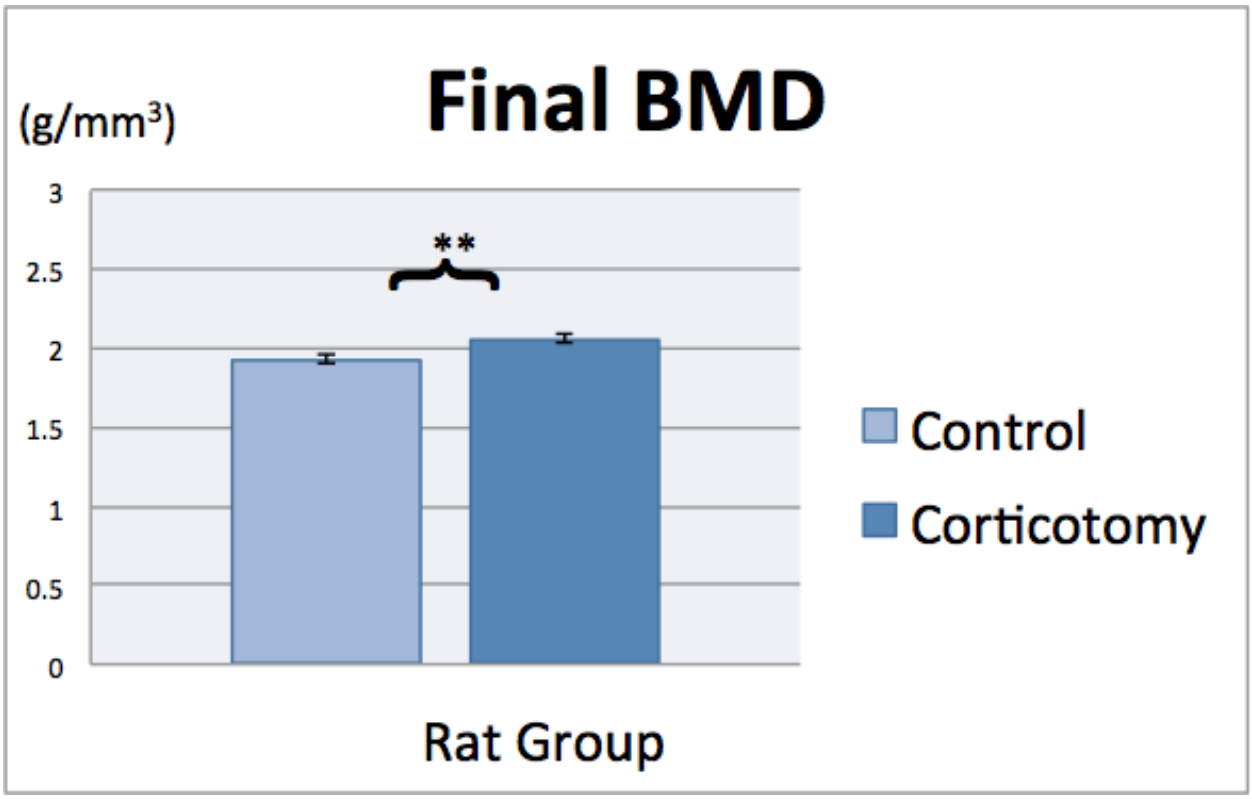

Fig. 9b: Average Results for BMD Analysis: The corticotomy side showed 10% greater BMD compared to the control side at 21 days. ** $p < .01$

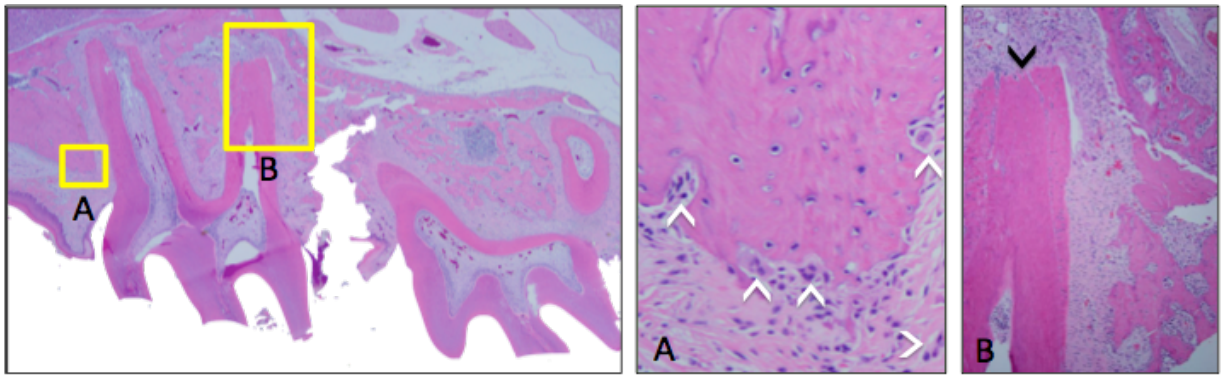

Fig. 10a: Corticotomy Side: Interradicular trabecular bone height shortened indicating moderate bone loss. **A)** Increased number of osteoclasts (white arrows) detected on compression side. **B)** Root apex is blunted (black arrow) due to moderate root resorption.

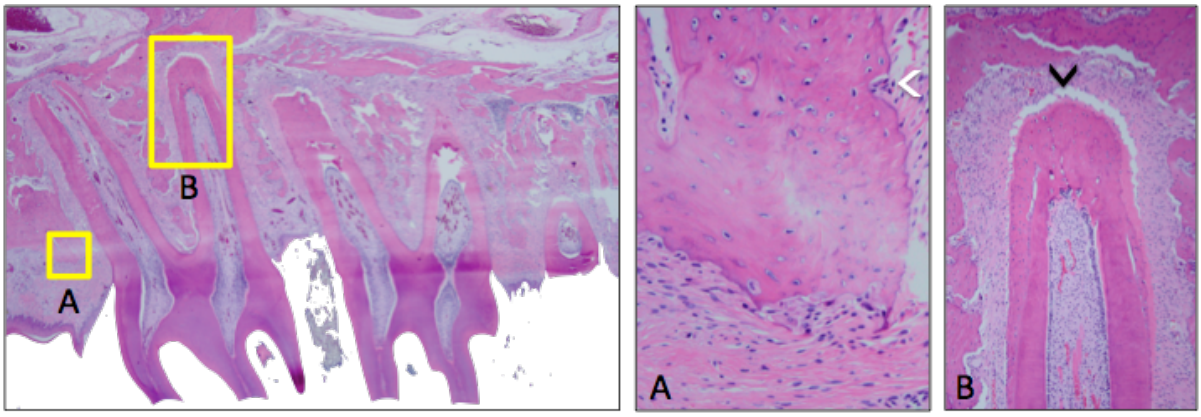

Fig. 10b: Control Side: Interradicular trabecular bone height appears normal indicating minimal bone loss. **A)** Mild numbers of osteoclasts (white arrow) detected on compression side. **B)** Root apex is well-defined (black arrow) indicating no root resorption.

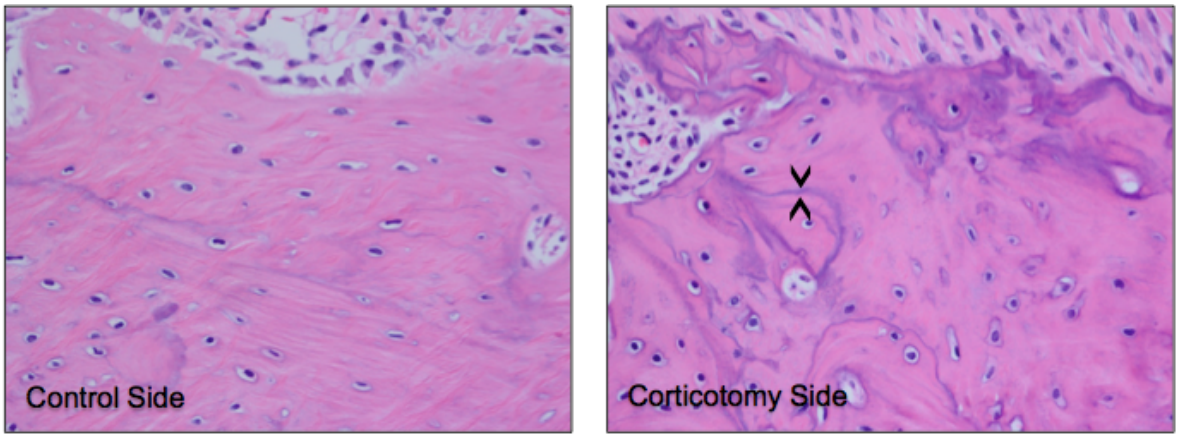

Fig. 11: Corticotomy vs Control Side Bone: Dark blue lines (black arrows) in the corticotomy side represents "new" or woven bone, which is a sign of increased bone metabolic activity. Woven bone is less organized than the mature, lamellar bone, which predominates in the control side.

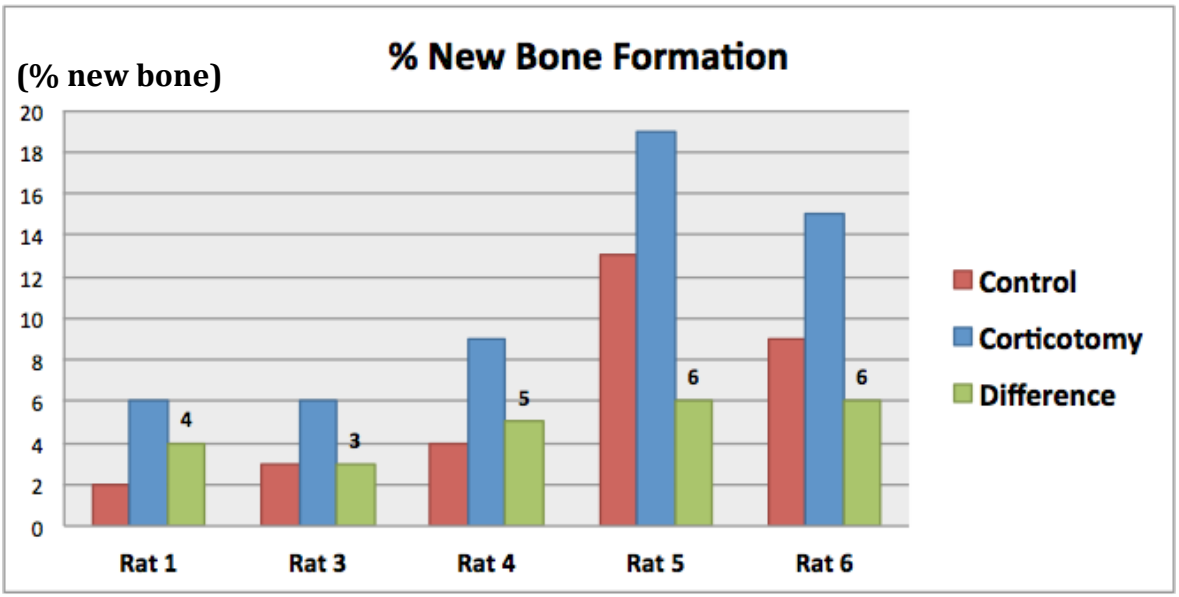

Fig. 12: New Bone Quantification: 3% to 6% greater new bone formation observed on corticotomy side in all animals.

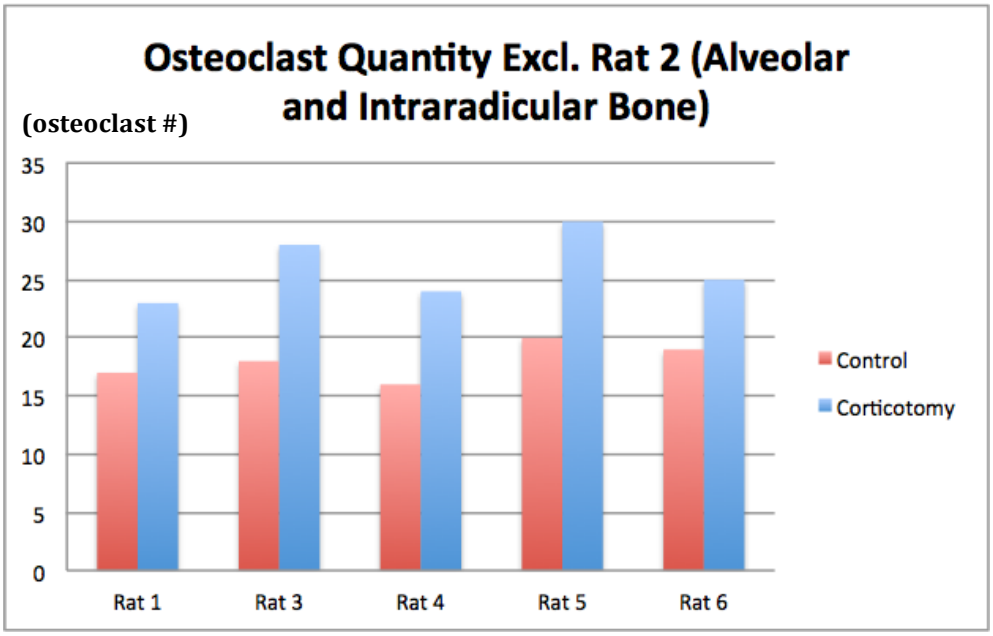

Fig. 13a: Osteoclast Quantification for Alveolar and Intraradicular Bone: Greater osteoclast quantity observed on corticotomy side across all animals.

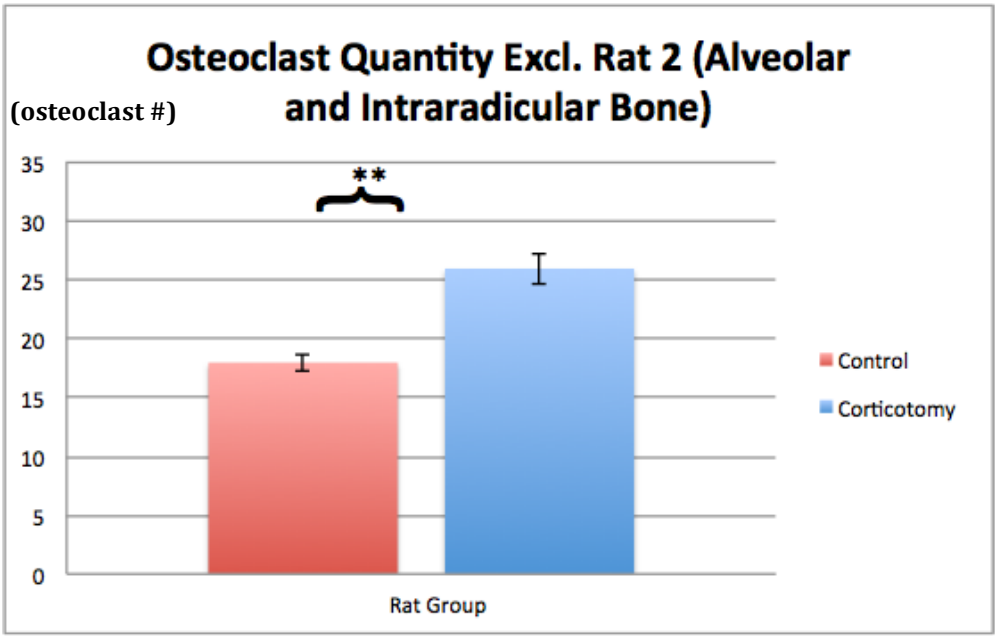

Fig. 13b: Average Osteoclast Quantification for Alveolar and Intraradicular Bone: 44% more osteoclasts observed on corticotomy side than control side.

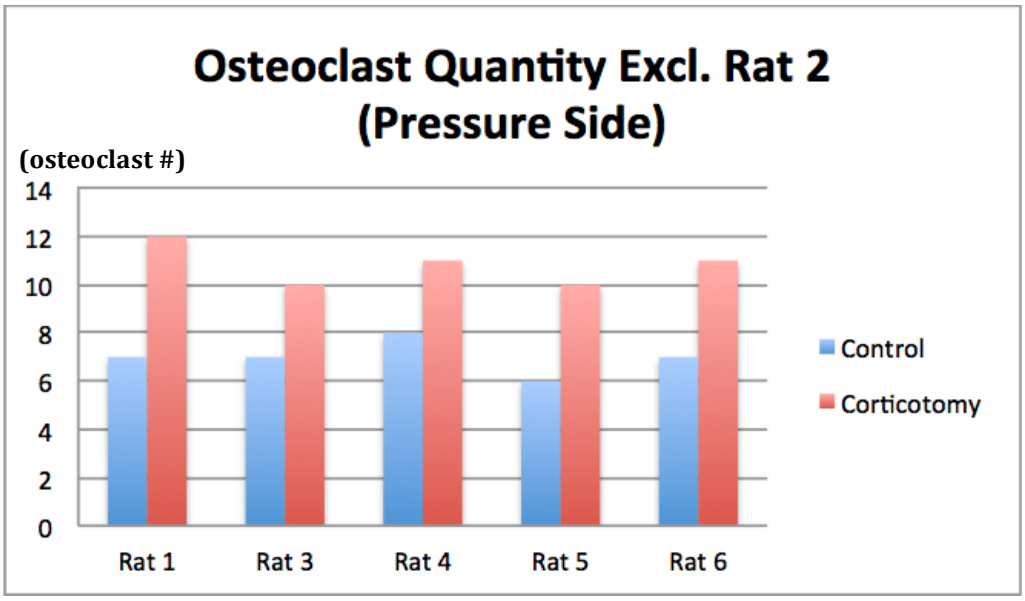

Fig. 14a: Osteoclast Quantification for Pressure Side: Greater osteoclast quantity observed on corticotomy side in all animals.

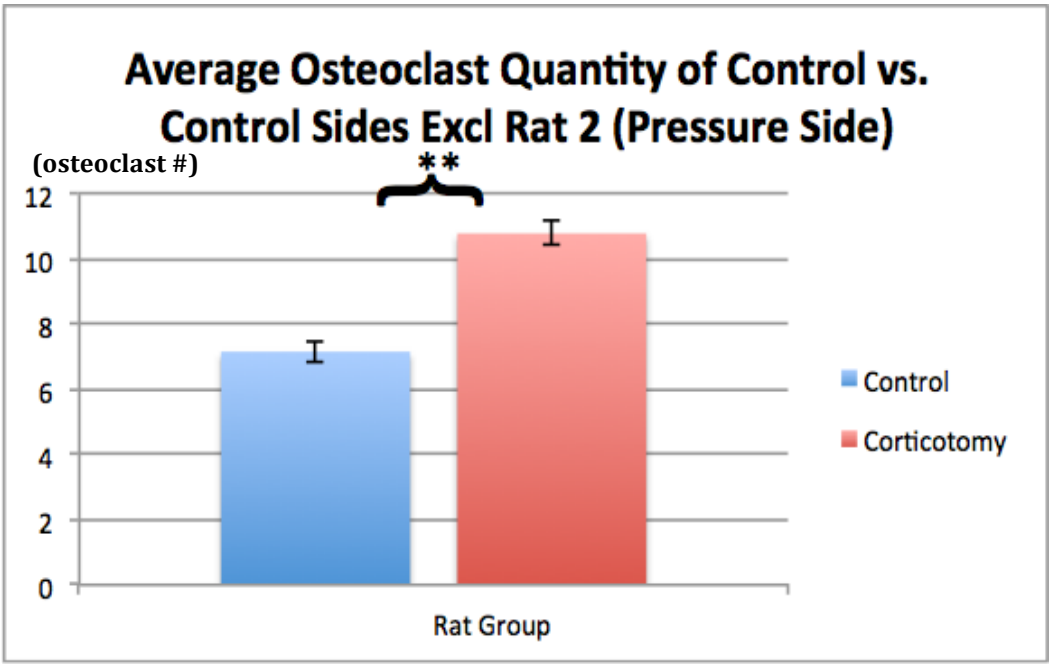

Fig. 14b: Average Osteoclast Quantification for Pressure Side: 55% greater osteoclast quantity observed on corticotomy side.

G: BIBLIOGRAPHY

1. Aerssens J, Boonen S, Lowet G, Dequeker J. Interspecies differences in bone composition, density, and quality: potential implications for in vivo bone research. Endocrinology 1998;139(2):663-70.
2. Alikhani M, Raptis M, Zoldan B, Sangsuwon C, Lee YB, Alyami B, et al. Effect of micro-osteoperforations on the rate of tooth movement. Am J Orthod Dentofacial Orthop 2013;144(5):639-48.
3. Andrade Jr. I, Taddei S, Souza P. Inflammation and Tooth Movement: The Role of Cytokines, Chemokines, and Growth Factors. Seminars in Orthodontics 2012;18(4):257-269.
4. Anholm JM, Crites DA, Hoff R, Rathbun WE. Corticotomy-facilitated orthodontics. CDA J 1986;14(12):7-11.
5. Baloul SS, Gerstenfeld LC, Morgan EF, Carvalho RS, Van Dyke TE, Kantarci A. Mechanism of action and morphologic changes in the alveolar bone in response to selective alveolar decortication-facilitated tooth movement. Am J Orthod Dentofacial Orthop 2011;139(4 Suppl):S83-101.
6. Bogoch E, Gschwend N, Rahn B, Moran E, Perren S. Healing of cancellous bone osteotomy in rabbits--Part I: Regulation of bone volume and the regional acceleratory phenomenon in normal bone. J Orthop Res 1993;11(2):285-91.
7. Buschang P, Campbell P, Ruso S. Accelerating Tooth Movement With Corticotomies: Is It Possible and Desirable? Seminars in Orthodontics 2012;18(4):286-294.
8. Cirelli JA, Cirelli CC, Holzhausen M, Martins LP, Brandao CH. Combined periodontal, orthodontic, and restorative treatment of pathologic migration of anterior teeth: a case report. Int J Periodontics Restorative Dent 2006;26(5):501-6.
9. Darendeliler MA, Zea A, Shen G, Zoellner H. Effects of pulsed electromagnetic field vibration on tooth movement induced by magnetic and mechanical forces: a preliminary study. Aust Dent J 2007;52(4):282-7.
10. Deguchi T, Takano-Yamamoto T, Yabuuchi T, Ando R, Roberts WE, Garetto LP. Histomorphometric evaluation of alveolar bone turnover between the maxilla and the mandible during experimental tooth movement in dogs. Am J Orthod Dentofacial Orthop 2008;133(6):889-97.
11. Delabarre CF. Odontologie ou Observations sans les Dents Humaines. Paris 1815.
12. Delaisse JM, Engsig MT, Everts V, del Carmen Ovejero M, Ferreras M, Lund L, et al. Proteinases in bone resorption: obvious and less obvious roles. Clin Chim Acta 2000;291(2):223-34.
13. Dibart S, Sebaoun JD, Surmenian J. Piezocision: a minimally invasive, periodontally accelerated orthodontic tooth movement procedure. Compend Contin Educ Dent 2009;30(6):342-4, 346, 348-50.
14. Dibart S, Yee C, Surmenian J, Sebaoun JD, Baloul S, Goguet-Surmenian E, et al. Tissue response during Piezocision-assisted tooth movement: a histological study in rats. Eur J Orthod 2013.
15. Dimitriou R, Tsiridis E, Giannoudis PV. Current concepts of molecular aspects of bone healing. Injury 2005;36(12):1392-404.
16. Dorfman HS, Turvey TA. Alterations in osseous crestal height following interdental osteotomies. Oral Surg Oral Med Oral Pathol 1979;48(2):120-5.

17. Doshi-Mehta G, Bhad-Patil WA. Efficacy of low-intensity laser therapy in reducing treatment time and orthodontic pain: a clinical investigation. Am J Orthod Dentofacial Orthop 2012;141(3):289-97.
18. Frost HM. The regional acceleratory phenomenon: a review. Henry Ford Hosp Med J 1983;31(1):3-9.
19. Gantes B, Rathbun E, Anholm M. Effects on the periodontium following corticotomy-facilitated orthodontics. Case reports. J Periodontol 1990;61(4):234-8.
20. Hagg U, Kaveewatcharanont P, Samaranayake YH, Samaranayake LP. The effect of fixed orthodontic appliances on the oral carriage of Candida species and Enterobacteriaceae. Eur J Orthod 2004;26(6):623-9.
21. Hamp SE, Lundstrom F, Nyman S. Periodontal conditions in adolescents subjected to multiband orthodontic treatment with controlled oral hygiene. Eur J Orthod 1982;4(2):77-86.
22. Hassan AH, Al-Fraidi AA, Al-Saeed SH. Corticotomy-assisted orthodontic treatment: review. Open Dent J 2010;4:159-64.
23. Henneman S, Von den Hoff JW, Maltha JC. Mechanobiology of tooth movement. Eur J Orthod 2008;30(3):299-306.
24. Iglesias-Linares A, Yanez-Vico RM, Moreno-Fernandez AM, Mendoza-Mendoza A, Solano-Reina E. Corticotomy-assisted orthodontic enhancement by bone morphogenetic protein-2 administration. J Oral Maxillofac Surg 2012;70(2):e124-32.
25. Iino S, Sakoda S, Ito G, Nishimori T, Ikeda T, Miyawaki S. Acceleration of orthodontic tooth movement by alveolar corticotomy in the dog. Am J Orthod Dentofacial Orthop 2007;131(4):448 e1-8.
26. Jager A, Zhang D, Kawarizadeh A, Tolba R, Braumann B, Lossdorfer S, et al. Soluble cytokine receptor treatment in experimental orthodontic tooth movement in the rat. Eur J Orthod 2005;27(1):1-11.
27. Kale S, Kocadereli I, Atilla P, Asan E. Comparison of the effects of 1,25 dihydroxycholecalciferol and prostaglandin E2 on orthodontic tooth movement. Am J Orthod Dentofacial Orthop 2004;125(5):607-14.
28. Kanzaki H, Chiba M, Arai K, Takahashi I, Haruyama N, Nishimura M, et al. Local RANKL gene transfer to the periodontal tissue accelerates orthodontic tooth movement. Gene Ther 2006;13(8):678-85.
29. Kawakami M. [Effects of local application of 1,25 (OH)2D3 on experimental tooth movement in rats]. Osaka Daigaku Shigaku Zasshi 1990;35(1):128-46.
30. Kawasaki K, Shimizu N. Effects of low-energy laser irradiation on bone remodeling during experimental tooth movement in rats. Lasers Surg Med 2000;26(3):282-91.
31. Kim SJ, Moon SU, Kang SG, Park YG. Effects of low-level laser therapy after Corticision on tooth movement and paradental remodeling. Lasers Surg Med 2009;41(7):524-33.
32. Kim YS, Kim SJ, Yoon HJ, Lee PJ, Moon W, Park YG. Effect of piezopuncture on tooth movement and bone remodeling in dogs. Am J Orthod Dentofacial Orthop 2013;144(1):23-31.
33. Kirschneck C, Proff P, Fanghaenel J, Behr M, Wahlmann U, Roemer P. Differentiated analysis of orthodontic tooth movement in rats with an improved rat model and three-dimensional imaging. Ann Anat 2013;195(6):539-53.
34. Kole H. Surgical operations on the alveolar ridge to correct occlusal abnormalities. Oral Surg Oral Med Oral Pathol 1959;12(3):277-88 contd.
35. Kole H. Surgical operations on the alveolar ridge to correct occlusal abnormalities. Oral Surg Oral Med Oral Pathol 1959;12(4):413-20 contd.

36. Kole H. Surgical operations on the alveolar ridge to correct occlusal abnormalities. Oral Surg Oral Med Oral Pathol 1959;12(5):515-29 concl.
37. Kwon HJ, Pihlstrom B, Waite DE. Effects on the periodontium of vertical bone cutting for segmental osteotomy. J Oral Maxillofac Surg 1985;43(12):952-5.
38. Lee W, Karapetyan G, Moats R, Yamashita DD, Moon HB, Ferguson DJ, et al. Corticotomy-/osteotomy-assisted tooth movement microCTs differ. J Dent Res 2008;87(9):861-7.
39. Mathews DP, Kokich VG. Accelerating tooth movement: The case against corticotomy-induced orthodontics. American Journal of Orthodontics and Dentofacial Orthopedics 2013;144(1):5-13.
40. McDonald F. Electrical effects at the bone surface. Eur J Orthod 1993;15(3):175-83.
41. Murphy KG, Wilcko MT, Wilcko WM, Ferguson DJ. Periodontal accelerated osteogenic orthodontics: a description of the surgical technique. J Oral Maxillofac Surg 2009;67(10):2160-6.
42. Okada Y, Naka K, Kawamura K, Matsumoto T, Nakanishi I, Fujimoto N, et al. Localization of matrix metalloproteinase 9 (92-kilodalton gelatinase/type IV collagenase = gelatinase B) in osteoclasts: implications for bone resorption. Lab Invest 1995;72(3):311-22.
43. Ozturk M, Doruk C, Ozec I, Polat S, Babacan H, Bicakci AA. Pulpal blood flow: effects of corticotomy and midline osteotomy in surgically assisted rapid palatal expansion. J Craniomaxillofac Surg 2003;31(2):97-100.
44. Park Y-G, Kang S-G, Kim S-J. Accelerated tooth movement by Corticision as an osseous orthodontic paradigm. Kinki Tokai Kyosei Shika Gakkai Gakujyutsu Taikai, Sokai 2006;48:1.
45. Penarrocha-Diago M, Rambla-Ferrer J, Perez V, Perez-Garrigues H. Benign paroxysmal vertigo secondary to placement of maxillary implants using the alveolar expansion technique with osteotomes: a study of 4 cases. Int J Oral Maxillofac Implants 2008;23(1):129-32.
46. Proffit WR, Fields HW. Contemporary orthodontics. 3rd ed. St. Louis: Mosby; 2000.
47. Ren A, Lv T, Kang N, Zhao B, Chen Y, Bai D. Rapid orthodontic tooth movement aided by alveolar surgery in beagles. Am J Orthod Dentofacial Orthop 2007;131(2):160 e1-10.
48. Ren Y, Maltha JC, Kuijpers-Jagtman AM. Optimum force magnitude for orthodontic tooth movement: a systematic literature review. Angle Orthod 2003;73(1):86-92.
49. Ren Y, Maltha JC, Kuijpers-Jagtman AM. The rat as a model for orthodontic tooth movement--a critical review and a proposed solution. Eur J Orthod 2004;26(5):483-90.
50. Roberts-Harry D, Sandy J. Orthodontics. Part 11: orthodontic tooth movement. Br Dent J 2004;196(7):391-4; quiz 426.
51. Roblee RD, Bolding SL, Landers JM. Surgically facilitated orthodontic therapy: a new tool for optimal interdisciplinary results. Compend Contin Educ Dent 2009;30(5):264-75; quiz 276, 278.
52. Sebaoun JD, Kantarci A, Turner JW, Carvalho RS, Van Dyke TE, Ferguson DJ. Modeling of trabecular bone and lamina dura following selective alveolar decortication in rats. J Periodontol 2008;79(9):1679-88.
53. Seifi M, Shafeei HA, Daneshdoost S, Mir M. Effects of two types of low-level laser wave lengths (850 and 630 nm) on the orthodontic tooth movements in rabbits. Lasers Med Sci 2007;22(4):261-4.
54. Soma S, Iwamoto M, Higuchi Y, Kurisu K. Effects of continuous infusion of PTH on experimental tooth movement in rats. J Bone Miner Res 1999;14(4):546-54.

55. Sun X, Zhu X, Xu C, Ye N, Zhu H. [Effects of low energy laser on tooth movement and remodeling of alveolar bone in rabbits]. Hua Xi Kou Qiang Yi Xue Za Zhi 2001;19(5):290-3.
56. Teixeira CC, Khoo E, Tran J, Chartres I, Liu Y, Thant LM, et al. Cytokine expression and accelerated tooth movement. J Dent Res 2010;89(10):1135-41.
57. Teng GY, Liou EJ. Interdental osteotomies induce regional acceleratory phenomenon and accelerate orthodontic tooth movement. J Oral Maxillofac Surg 2014;72(1):19-29.
58. Topkara A, Karaman AI, Kau CH. Apical root resorption caused by orthodontic forces: A brief review and a long-term observation. Eur J Dent 2012;6(4):445-53.
59. Truchot G. [Do multi-bracket orthodontic appliances favor the development of parasites and fungi in the oral environment? Pathological and therapeutic consequences]. Orthod Fr 1991;62 Pt 3:1019-24.
60. Twaddle BA FD, Wilcko WM, et al. Dento-alveolar bone density changes following accelerated orthodontics. J Dent Res. 2002;80:301.
61. Wang L, Lee W, Lei DL, Liu YP, Yamashita DD, Yen SL. Tisssue responses in corticotomy- and osteotomy-assisted tooth movements in rats: histology and immunostaining. Am J Orthod Dentofacial Orthop 2009;136(6):770 e1-11; discussion 770-1.
62. Wilcko MT, Wilcko WM, Pulver JJ, Bissada NF, Bouquot JE. Accelerated osteogenic orthodontics technique: a 1-stage surgically facilitated rapid orthodontic technique with alveolar augmentation. J Oral Maxillofac Surg 2009;67(10):2149-59.
63. Wood DL, Hoag PM, Donnenfeld OW, Rosenfeld LD. Alveolar crest reduction following full and partial thickness flaps. J Periodontol 1972;43(3):141-4.
64. Yamaguchi M, Hayashi M, Fujita S, Yoshida T, Utsunomiya T, Yamamoto H, et al. Low-energy laser irradiation facilitates the velocity of tooth movement and the expressions of matrix metalloproteinase-9, cathepsin K, and alpha(v) beta(3) integrin in rats. Eur J Orthod 2010;32(2):131-9.
65. Zahrowski J, Jeske A. Apical root resorption is associated with comprehensive orthodontic treatment but not clearly dependent on prior tooth characteristics or orthodontic techniques. J Am Dent Assoc 2011;142(1):66-8.